

UNIVERSITY OF OKLAHOMA

GRADUATE COLLEGE

MAKING SATELLITE SENSORS BETTER FOR HYDROCLIMATIC
APPLICATIONS: EVALUATION OF NASA SMAP SOIL MOISTURE USING
OKLAHOMA'S ENVIRONMENTAL MONITORING NETWORK—MESONET

A THESIS

SUBMITTED TO THE GRADUATE FACULTY

in partial fulfillment of the requirements for the

Degree of

MASTER OF ENVIRONMENTAL SCIENCE

By

CHEN XU
Norman, Oklahoma
2017

MAKING SATELLITE SENSORS BETTER FOR HYDROCLIMATIC
APPLICATIONS: EVALUATION OF NASA SMAP SOIL MOISTURE USING
OKLAHOMA'S ENVIRONMENTAL MONITORING NETWORK—MESONET

A THESIS APPROVED FOR THE
SCHOOL OF CIVIL ENGINEERING AND ENVIRONMENTAL SCIENCE

BY

Dr. Yang Hong, Chair

Dr. David Sabatini

Dr. Ke Zhang

© Copyright by CHEN XU 2017
All Rights Reserved.

Acknowledgements

I would like to sincerely thank Dr. Yang Hong, for his immense time and enormous efforts to bring me into the world of scientific research remote sensing hydrology. As an innocent transfer student from biology, I had no clue what the scope of engineering is, not to mention working with satellite data. It was Dr. Hong's work and diligence that set me a role model to work rigorously yet effectively and tirelessly. He wholeheartedly helped me data analysis and manuscript revision, step by step and even hand by hand. Without his generous help and supervision, this thesis would not have been possible.

I am very grateful to Dr. David Sabatini, who has enlightened my passion and hope through his vivid class. I was frustrated with catching up with the engineering classes and hard-core sciences research by the time, and Dr. Sabatini's WaTER for Emerging Regions course made me believe once more that what I'm learning can help those in need. The final project for his class working on hygiene and sanitation in rural Bangladesh has opened my eyes to get involved with the sustainable development, which I firmly believe will be the route for my future endeavor.

I very much appreciate for the dedication by Dr. Ke Zhang as my committee member, to provide me with the scope, plan, and hands-on meticulous guidance for data searching and processing. His tireless hustling and reminding prevented me from stagnating. It was not only academics but also how to interact with people in academia, that I learned from him.

I would also like to acknowledge Dr. Jeffery Basara for generously provide precious research data for us graduate students, as one of the founders of renowned

Oklahoma Mesonet. He has also provided me with opportunities such as MOISST symposium in the field of soil moisture, which shared me with vast connections and knowledge within the field.

Special thanks goes to everyone in my lab, it is their friendly and critical advices that have been greatly improved my graduate study and this very thesis. In particular, I gratefully thank Dr. Emad Hasan, for solving my technical difficulties for ArcGIS and for modifying my abstract; also our fellow visiting PhD student Dr. Yi Liu, for helping me with coding with MATLAB for data extraction. Acknowledgment also goes to other lab mates, Zhen Hong, Drs. Xianwu Xue, and Yixin Wen, as well as HyDROS group visiting scholars throughout the years Chunfen Zeng, Xiaona Zhang, Yan Shen, Wenyu Yang, Haijun Liu, Jinping Zhang, Na Yang, Yan Ye, Yong Ye, and Bin Yang for supporting me academically and spiritually during the whole course of my graduate study.

This master's thesis cannot be fulfilled without my English writing tutor, Jessica Reynolds, the Director of English Training and Certification Services at OU. She has gone through my writing for the first draft, corrected grammatical errors, and provided with me valuable suggestions for improving manuscript.

Last, but far from the least, I would like to my family for supporting me whole heartedly. My parents pointed me to the direction of hydrology, an area very much in need, and their thoughtful care and love has moved me forward. My significant other, Iris Xiaoshuang Luo, has always been by my side through ups and downs, strongly academically and spiritually supportive, improving ourselves together, and hope for the future. It is clear that they are the real force behind me.

Table of Contents

Acknowledgements	iv
List of Tables	viii
List of Figures.....	ix
Abstract.....	xi
Chapter 1: Introduction.....	1
2.1 Surface Soil Moisture vs. Remote Sensing Techniques	2
2.1.1 Measurement of Surface Soil Moisture	2
2.1.2 Soil Moisture in the Scope of Hydrology	2
2.1.3 Application of Remote Sensing Techniques in Surface Soil Moisture Measurement	3
2.1.4 Passive Microwave Remote Sensing of Surface Soil Moisture	4
2.1.5 NASA’s SMAP (Soil Moisture Active Passive) Mission	5
2.1.6 Oklahoma Mesonet.....	5
2.2 Statement of Problem	8
2.3 Objectives.....	9
2.4 Hypotheses	10
Chapter 2: Spatiotemporal Variation of Soil Moisture in Oklahoma.....	11
2.1 Study Area: State of Oklahoma.....	11
2.1.1 Geographical Condition of Oklahoma.....	11
2.1.2 Climatic Condition of Oklahoma	12
2.2 Datasets.....	13
2.2.1 SMAP Soil Moisture Data.....	13

2.2.2 Mesonet Ground Observation Data	14
2.3 Methods	15
2.3.1 Spatial Downscaling Method for Remotely Sensed SMAP Data	16
2.3.2 Spatial Interpolation Method for Point-based Mesonet Data	16
2.3.3 Evaluation of Remotely Sensed SMAP Data with in situ Mesonet Observations	17
2.3.4 Spatial Variation Pattern: Precipitation, Temperature, and Climatic Inference	18
2.3.5 Temporal Variation Pattern: Seasonal Variability	21
Chapter 3. Comparison of SMAP Passive and Mesonet Soil Moisture	22
3.1 Spatial Variation in Oklahoma Soil Moisture based on Mesonet Data	22
3.2 Temporal Variation in Oklahoma Soil Moisture	27
Chapter 4. Spatial Analysis of the SMAP Soil Moisture Comparing to the Mesonet Observations	29
4.1 Statewide Comparison of SMAP and Mesonet Soil Moisture	29
4.2 Evaluation of SMAP based on Climatic Conditions	34
4.2.1 SMAP Evaluation based on Precipitation Zones	34
4.2.2 SMAP Evaluation based on Temperature Zones	39
4.2.3 SMAP Evaluation based on Climatic Divisions	45
Chapter 5. Temporal Analysis of SMAP Soil Moisture: <i>Seasonality</i>	52
Chapter 6. Summary, Conclusions and Future Work	56
6.1 Summary and Conclusions	56
6.2 Future Work	58

List of Tables

Table 1 List of Major Current Remote Sensing Instruments and Satellite Platforms for Global Soil Moisture Observation.....	4
Table 2 List of SMAP Baseline Science Data Products (from SMAP website)	14

List of Figures

Figure 1 A Standard Mesonet Station (from Mesonet website).....	6
Figure 2 Distribution of Oklahoma Mesonet Sites.....	7
Figure 3 Side View of a Typical Oklahoma Mesonet Station (from Mesonet website) ..	7
Figure 4 Surface Upward Microwave Emission (Neelam et al., 2015).....	9
Figure 5 Location of the State of Oklahoma within the United States.....	11
Figure 6 Average Annual Temperature and Average Annual Precipitation of Oklahoma (Keller, 2008)	13
Figure 7 Oklahoma Precipitation Zones.....	19
Figure 8 Oklahoma Temperature Zones.....	20
Figure 9 Oklahoma Climate Divisions	21
Figure 10 Average Monthly Surface Soil Moisture (Mesonet, top 5 cm).....	24
Figure 11 Longitudinal and Latitudinal Distributions of Mesonet Surface SM.....	24
Figure 12 Spatially Interpolated Mesonet Average Monthly Surface Soil Moisture.....	26
Figure 13 Time Series Analysis of Soil Moisture as a Function of Precipitation and Temperature for State-as-a-Whole	27
Figure 14 Downscaled SMAP Average Monthly Surface Soil Moisture.....	30
Figure 15 Statewide SMAP versus Mesonet Average Monthly Surface Soil Moisture for the First 12 Months, the Last 12 Months, and the Entire 16 Month.....	32
Figure 16 Statistics for SMAP – Mesonet Correlation Statewide	33
Figure 17 Time Series Analysis of Soil Moisture based on Precipitation Zones.....	35
Figure 18 Box-and-Whisker Diagram for Each Precipitation Zone.....	37
Figure 19 Statistics of SMAP – Mesonet Correlation for Each Precipitation Zone.....	38

Figure 20 Time Series Analysis of Soil Moisture based on Temperature Zones	40
Figure 21 Box-and-Whisker Diagram for Each Temperature Zone.....	42
Figure 22 Statistics of SMAP – Mesonet Correlation for Each Temperature Zone.....	43
Figure 23 Time Series Analysis of Soil Moisture based on Climatic Regions	47
Figure 24 Box-and-Whisker Diagram for Each Climatic Region	49
Figure 25 Statistics of SMAP – Mesonet Correlation for Each Climatic Region	50
Figure 26 Average Seasonal Surface Soil Moisture Distribution	52
Figure 27 Box-and-Whisker Diagram for Each Season	53
Figure 28 Statistics for SMAP – Mesonet Correlation Statewide	55

Abstract

Soil moisture, quantified as the ratio of liquid water to soil in volume or weight, is the measurement of the water that is held in the space between soil particles. Understanding the components of soil, particularly its water concentration, is an important aspect of the hydrological cycle. This concept is key in understanding the relationship of the circulation pathway of water and heat as they travel between Earth's surface and then the atmosphere. This interaction has a great impact on weather, ecosystems and their climates. Advances in remote sensing, particularly microwave remote sensing, have provided significant information on soil water content. If coupled with geographic pieces of information such as soil types and topographical details, it may be able to provide accurate data on soil water content on a global basis. National Aeronautics and Space Administration (NASA)'s Soil Moisture Active Passive (SMAP) mission takes place in an orbiting observatory that measures the amount of water in the top 10 cm of soil on Earth's surface every 2 – 3 days since 2015. Environmental factors including precipitation, temperature, vegetation cover, soil properties (density and texture), and surface roughness may all affect the accuracy of the remotely sensed soil moisture measurement. There being so many variables that can affect data, it is critical to compare SMAP soil moisture data with in situ observations for sensor calibration and hydrometeorological applications.

The objective of this study is to evaluate the potential utility of the surface soil moisture data retrieved from remote sensing techniques, those derived from SMAP satellites in particular, by comparing them with the ground-observed data of the Oklahoma Mesonet that monitors a number of atmospheric and hydrologic variables,

including solar radiation, humidity, temperature, wind speed and direction, and soil moisture. This data will aid in operational weather forecasting and environmental research across the state. First, the spatiotemporal variation pattern of statewide soil moisture is described with site-wise monthly average Mesonet data from the top 5, 25, and 60 cm of soil respectively. This would then show the correlation between the remotely-sensed SMAP soil moisture data and Mesonet soil moisture observations at three soil depths, both spatially – statewide, as well as regions of three precipitation zones, three temperature zones, and nine climatic zones, and temporally – for each season. Three specific hypotheses and findings will be made and reached. First, the remotely sensed SMAP retrievals relatively fit and correlate well with Mesonet data. Spatially, the wetter and warmer climatic regions have a higher correlation and lower error in the SMAP soil moisture. During the summer and winter for short periods, the SMAP soil moisture data has a greater degree of deviations to the observations than in the other times of the year. Second, the Mesonet data of the top 5 cm of soil shows the best correlation with the SMAP information. This reconfirms the remotely sensed SMAP data validity for measuring top soil layer than root zone soil moisture. Third and lastly, the SMAP soil moisture closely corresponds with environmental conditions. This is especially pertinent with precipitation events and temperature variations. This study proves the hypotheses and concludes that the remotely sensed soil moisture data retrieved from SMAP is considered to be effective in observing land surface soil moisture data in Oklahoma. Furthermore, the quantitative findings support electrical engineers to calibrate the errors in remote sensing signals and retrieval algorithms, and thus to develop more functional satellite sensors for future missions.

Chapter 1: Introduction

Advances in remote sensing have provided the means to observe state variables from space at large scales, thereby improving our understanding of many hydrological processes. Soil moisture, the amount of water that is held in the spaces between soil particles, is measured as the ratio of liquid water content to soil in volume or weight. As an important component of hydrological cycle, soil moisture information is key to understanding the flows of water and heat energy between the Earth's surface and atmosphere that impact weather, water and climate. The operational soil moisture information certainly contributes to improving hydrological modeling and numerical weather forecasting (NWF), drought/flood monitoring and forecasting, and climate studies (Fan, 2004). Surface soil moisture information can be retrieved globally at real time from space-borne remote sensing with the improvements of passive microwave remote sensors, which have promoted their utilities in monitoring surface moisture conditions. However, environmental factors such as precipitation, temperature, vegetation cover, soil properties (density and texture), and surface roughness can all obstruct the penetration of remote sensing signals to some degree, which will affect the measurement accuracy. Errors associated with both the modeling and the observations can be accounted for when updating model outputs by incorporating real time indirect (i.e., remotely sensed) observations into hydrological model simulation. The objective of this study is to evaluate the potential utility of the surface soil moisture data retrieved from remote sensing techniques, those derived from SMAP satellite in particular, by comparing them with ground-observed Oklahoma Mesonet data.

1.1 Surface Soil Moisture vs. Remote Sensing Techniques

1.1.1 Measurement of Surface Soil Moisture

Soil water is held in the pore space, or the cracks and empty spaces between soil particles. Soil moisture content typically takes up approximately 25% of the space in the soil, but also depends on soil types and varies between about 15% for sandy soil and up to 50% for clay. Monitoring soil moisture levels is required for effective irrigation water management, and useful for drought early warning, and flood warnings (McCorkle et al., 2016). Soil water content is most commonly expressed as the percent of water by weight, and determined by dividing the weight of the water in the soil by the dry weight of the soil. Ground measurement of soil moisture can be realized through gravimetric (weighing), radioactive (neutron probe), capacitive (soil probes or time domain reflectometry), conductivity (electrical resistance block sensors), soil suction techniques, and tensiometers or other portable measuring devices (Tian et al., 2016; Werner, 1992).

1.1.2 Soil Moisture in the Scope of Hydrology

According to Shen et al. (2013), in bare soil cases, independent parameters including moisture and soil roughness are the major variables to determine. In terms of hydrologic modeling and water resource management, estimating and characterizing surface soil moisture's spatiotemporal variability is especially crucial. "The availability of soil moisture affects plant production potential, rainfall runoff volume, and many other parameters that are of interest to agricultural production, forest management, soil conservation, and watershed management and modeling" (USGS). Furthermore, soil

moisture information is key to understanding the flows of water and heat energy between the surface and atmosphere that impact weather and climate as well, as the amount of water that evaporates from the land surface into the atmosphere depends on soil moisture.

1.1.3 Application of Remote Sensing Techniques in Surface Soil Moisture Measurement

Advances in remote sensing have provided the means to observe state variables from space at large scales, thereby improving our understanding of many hydrological processes (Schmugge et al., 2002). By taking advantage of the land surface emission characteristics, many state variables such as the land surface temperature, surface soil moisture, snow cover, and evapotranspiration, can be monitored by radiometers installed on satellites. Amongst these applications, microwave remote sensing of surface soil moisture is particularly important because of the many limitations on obtaining soil moisture through traditional field measurements (Gao, 2005). Converting spectral reflectance obtained from remotely sensed images may yield significant soil moisture information and, if augmented with geographic information such as soil types, land cover, land use, slope and terrain elevation, may provide accurate data on soil water content on a global basis (USGS). The operational soil moisture information would certainly contribute to improving hydrological modeling and numerical weather forecasting (NWF), drought/flood monitoring and forecasting, and climate studies. Errors associated with both the modeling and the observations can be accounted for when updating model outputs by incorporating real time indirect (i.e., remotely sensed) observations into hydrological models. For example, forcing errors (primarily precipitation errors) can be reduced by knowledge of the soil wetness monitored in real

time using the data assimilation technique (Entekhabi et al., 1999) to integrate remote sensing and land surface models to produce root zone soil moisture estimates, thus preventing temporal propagation of these errors through the model space.

1.1.4 Passive Microwave Remote Sensing of Surface Soil Moisture

The two unique advantages of passive microwave frequencies have promoted their utility in monitoring surface moisture conditions. Firstly, dielectric conductivity of the soil decreases with the increasing soil water content, resulting in reduced surface emission (or brightness temperature). The lower the frequency, the higher the sensitivity to soil moisture. Secondly, atmospheric contributions are minimal at many microwave frequencies such that land surface emission can penetrate through the atmosphere and thin clouds unaffected by atmospheric attenuation (Ulaby et al., 1986). As a result, surface soil moisture information can be retrieved globally in real time from spaceborne remote sensing (Gao, 2005). Table 1 lists the major current microwave remote sensing instruments and satellite platforms for global soil moisture observation.

Table 1 List of Major Current Remote Sensing Instruments and Satellite Platforms for Global Soil Moisture Observation

SM Products	Satellite Platform	Host	Launch Date	Spatial Resolution	Revisit Cycle	
AMSR-E	AQUA	JAXA	May 4, 2002	56 km	1 day	
AMSR-2	GCOM-W1		May 18, 2012	10 km	1 day	
SMOS	MIRAS	ESA	Nov 2009	10 km / 25 km	2-3 days	
SMAP	Active	SMAP	NASA	Oct 31, 2014	3 km	1-2 days
	Passive				36 km	

1.1.5 NASA's SMAP (Soil Moisture Active Passive) Mission

Launched in January 2015, Soil Moisture Active Passive (SMAP) is an orbiting observatory that measures the amount of water in the top 0 – 4 inches (0 – 10 centimeters) of soil everywhere on Earth's land surface every two to three days since 2015. SMAP was designed to provide high-resolution soil moisture information with radar (active) and radiometer (passive) which operate at L-band frequencies. Although a hardware mishap has failed the radar shortly after its launch, SMAP passive sensor has returned more than two years of soil moisture data that is critical for improving crop yield forecasts and irrigation planning around the world. Indirectly monitoring global food production will also allow SMAP to help improve targeting of humanitarian food assistance. Furthermore, as a deficit in the amount of moisture in the soil defines agricultural drought, SMAP's high fidelity measurements of soil moisture serve as a drought early warning, and improve flood warnings by assessing how wet the soil is before a rainstorm (SMAP).

1.1.6 Oklahoma Mesonet

The Oklahoma Mesonet, an abbreviation for “mesoscale” and “network”, is a world-class statewide network of environmental monitoring stations which was established in January 1994. It measures a wealth of atmospheric, hydrologic, and meteorological variables including temperature, humidity, solar radiation, wind speed and direction, and soil moisture to aid in operational weather forecasting and environmental research across the state (Brock et al. 1995; Oklahoma Mesonet 2008). With at least one station in each of Oklahoma's 77 counties, the Mesonet consists of

120 automated stations (Figure 1) across the state (Figure 2). Measurements are taken at a height of ten meters at each site with a set of instruments (Figure 3) including a lightning rod, a solar panel, a battery, a radio transmitter, a data logger and a rain gauge. Instruments that are located at every MESONET site and corresponding measured standard-primary variable for each instrument contain: RM Young Wind Monitor for wind speed; Thermometrics Air Temperature for air temperature; Vaisala Barometer for pressure; and Campbell Scientific 229-L for delta. These instruments' measurements are packaged into observations every 5 minutes, and then transmitted to the Oklahoma Climatological Survey (OCS) at the University of Oklahoma (OU), where the observed data are processed and verified for their quality, and then made public. The processing and verification are quick and only take approximately ten minutes from the time the measurements are made to when they become publically available. The facility is available 24-7 year-round for processing and quality control (Liu et al., 2011).



Figure 1 A Standard Mesonet Station (from Mesonet website)

Oklahoma Counties and Mesonet Sites

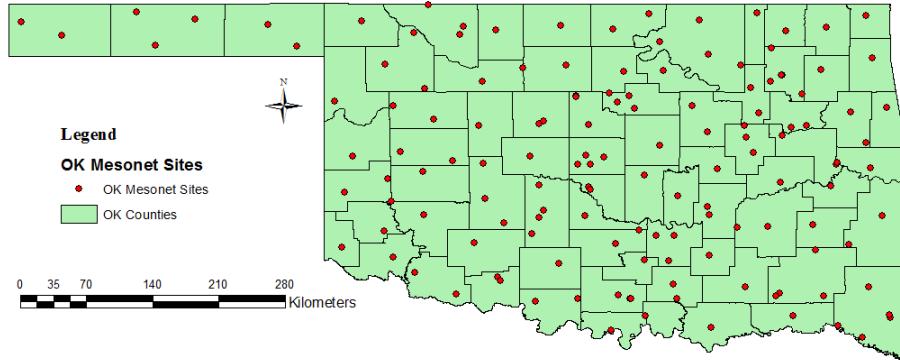


Figure 2 Distribution of Oklahoma Mesonet Sites

Side View of a Typical Mesonet Station

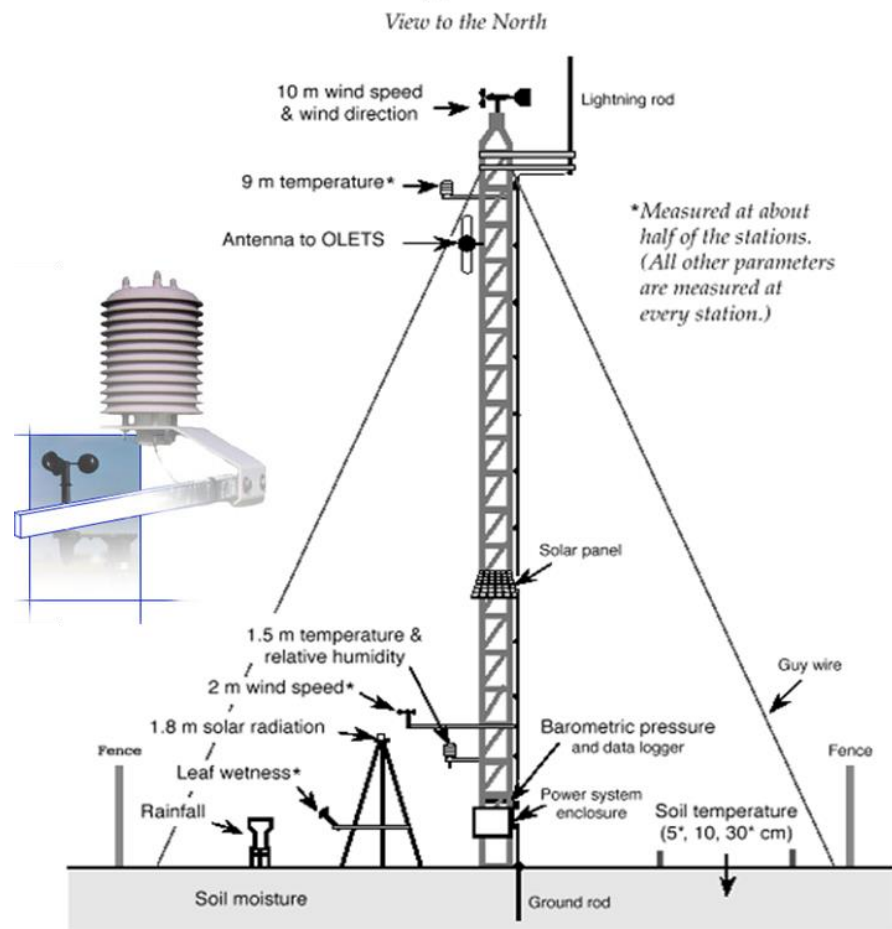


Figure 3 Side View of a Typical Oklahoma Mesonet Station (from Mesonet website)

1.2 Statement of Problem

Microwave remote sensing has been proven successful for examining dielectric conductivity of the soil based on the physical temperature and surface emissivity for soil water content measurement, but since the various algorithms used for different passive microwave sensors translate the thermal energy emission to brightness temperature which lead into variable soil moisture product quality and continuity across space and time. The SMAP satellite uses Radiative Transfer Model (RTM) for retrieving soil moisture, with its most widely used form (Mo et al., 1982) written as:

$$T_{B(p,f,\theta)} = e_{p,\theta} \cdot T_{eff} \cdot \exp\left(-\frac{\tau_{p,f}}{\cos\theta}\right) + T_C \cdot (1 - \omega_{p,f,\theta}) \cdot \left[1 - \exp\left(-\frac{\tau_{p,f}}{\cos\theta}\right)\right] + T_C \cdot \exp\left(-\frac{\tau_{p,f}}{\cos\theta}\right) \cdot (1 - \omega_{p,f,\theta}) \cdot \left[1 - \exp\left(-\frac{\tau_{p,f}}{\cos\theta}\right)\right] \cdot r_{p,f,\theta}$$

T_B is the brightness temperature of the soil surface, τ_p is the nadir optical depth, ω_p is the single scatter albedo, r_p is the rough surface reflectivity, T_{eff} and T_C are the effective physical temperatures of soil layers and vegetation, respectively.

This indicates that the SMAP sensor captures surface emissivity including: 1. upward soil emission, 2. upward vegetation emission, and 3. vegetation emission reflected by soil (Figure 4). But since vegetation scattering and absorption varies with hydroclimate and hence RTM is not optimum under highly heterogeneous landscape conditions (Neelam and Mohanty, 2015). Also, environmental factors such as precipitation, temperature, vegetation cover, soil properties (density and texture), and surface roughness can all obstruct the penetration of remote sensing signals to some degree, which will affect the measurement accuracy (Charpentier and Groffman, 1992).

Therefore evaluation of satellite soil moisture product is necessary to improve our understanding of the advantages and disadvantages of each sensor under different conditions across spatiotemporal scales.

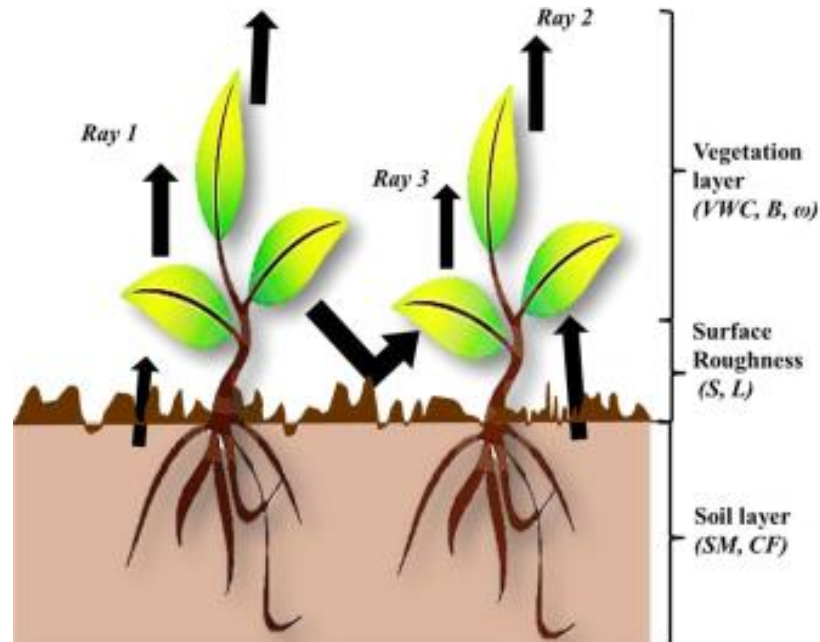


Figure 4 Surface Upward Microwave Emission (Neelam et al., 2015)

1.3 Objectives

The objective of this study is to evaluate the potential utility of the surface soil moisture data retrieved from remote sensing techniques, in particular those derived from the SMAP satellite. SMAP soil moisture data are compared with ground-observed Oklahoma Mesonet data by plotting the correlation of the data in time-series. The output of this work is aimed at assessing the effectiveness of remotely sensed data in observing earth surface hydro-climatological phenomenon, thus helping electrical engineers calibrate the error in remote sensing signals and retrieval signals, and thus to develop more functional satellite sensors for future satellite missions.

1.4 Hypotheses

The overarching goal of this study is to assess the effectiveness of remotely sensed surface soil moisture data retrieved from SMAP products by comparing with the ground site-based Mesonet soil moisture observations. Based on empirical knowledge of soil moisture, the following three hypotheses are to be investigated in this study:

Hypothesis 1: The high transparency of microwave signal to penetrate through vegetation canopy, along with the acute sensitivity to respond to soil moisture variations, allow the surface soil moisture data retrieved from remote sensing techniques, those derived from the SMAP satellite in particular, fit and be highly correlated with ground-observed Oklahoma Mesonet data.

Hypothesis 2: With the limitation of remote sensing signal penetration blockage by the ground, the Mesonet ground data of depth in 5 cm is predicted to have the best correlation with the SMAP data, which shows that the remote sensing SMAP data will be more valid for the top soil layer.

Hypothesis 3: The remotely sensed SMAP soil moisture is expected to correspond with changes in surface environmental conditions, especially with climatic events of precipitation and temperature variation.

Chapter 2: Spatiotemporal Variation of Soil Moisture in Oklahoma

2.1 Study Area: State of Oklahoma

The study area is located in the state of Oklahoma, USA (latitude: 33°37' N to 37° N; longitude: 94°26' W to 103° W). Oklahoma has irrigated agriculture, rain-fed agriculture, wetlands, and riparian vegetation, and it has an overall semi-arid climate with average annual precipitation of about 870 mm.

Location of the State of Oklahoma within the United States

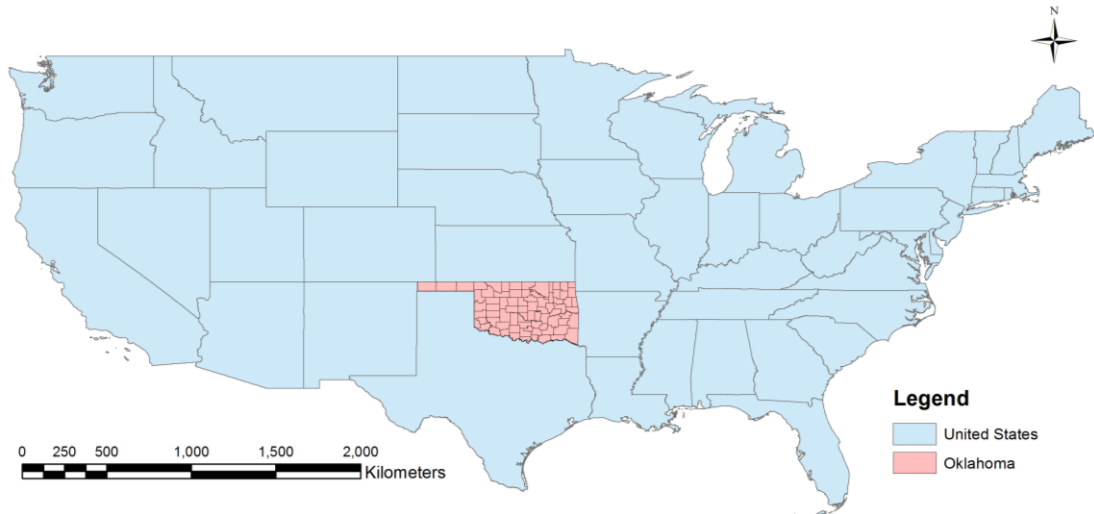


Figure 5 Location of the State of Oklahoma within the United States

2.1.1 Geographical Condition of Oklahoma

The state of Oklahoma lies in between the Great Plains and the Ozark Plateau and it occupies 69,898 square miles (181,035 km²), with 68,667 square miles (177,847 km²) of land and 1,281 square miles (3,188 km²) of water. The topography of the region generally slopes from high plains of Black Mesa complex in the west to the low wetlands of Arkansas River Basin in the east, with Ouachita Mountains in the southeast

and the Ozark Plateau in the northeast. Oklahoma lies entirely within the drainage basins of the Arkansas and Red Rivers, which is the two major tributaries of the Mississippi River.

2.1.2 Climatic Condition of Oklahoma

According to the Köppen climate classification, the state of Oklahoma lies in a transition zone of semi-arid climate in the west, humid continental climate to the north, and humid subtropical climate to the southeast (Peel et al., 2007). The frequent interactions between cold, dry air from the Great Plains in the north, warm, moist air from the Gulf of Mexico in the southeast, and hot, dry air from the southwest produce severe weather including thunderstorms and tornadoes remarkably during the months of May and June. The average annual temperature varies on the North-South gradient, whereas the average annual precipitation diverges vastly from low in the west to high in the east (Figure 6), making the state a perfect spot for climatological, meteorological, and hydrological observations and experiments. The average annual temperature ranges from 62 °F (17 °C) along the Red River on the southern border to 58 °F (14 °C) along the northern border, and further decreases to 54 °F (12 °C) on the tip of panhandle. The average annual precipitation, on the other hand, decreases sharply from 56 inches (1422 mm) in the southeast to 17 inches (431 mm) in the far western panhandle (Oklahoma Mesonet 2008). Another feature of precipitation in Oklahoma is strong seasonal variability. A significant portion of the state's precipitation is associated with thunderstorms. Due to the severe weather including thunderstorms and tornadoes during the months of May and June, summer precipitation is prevalently high across the state.

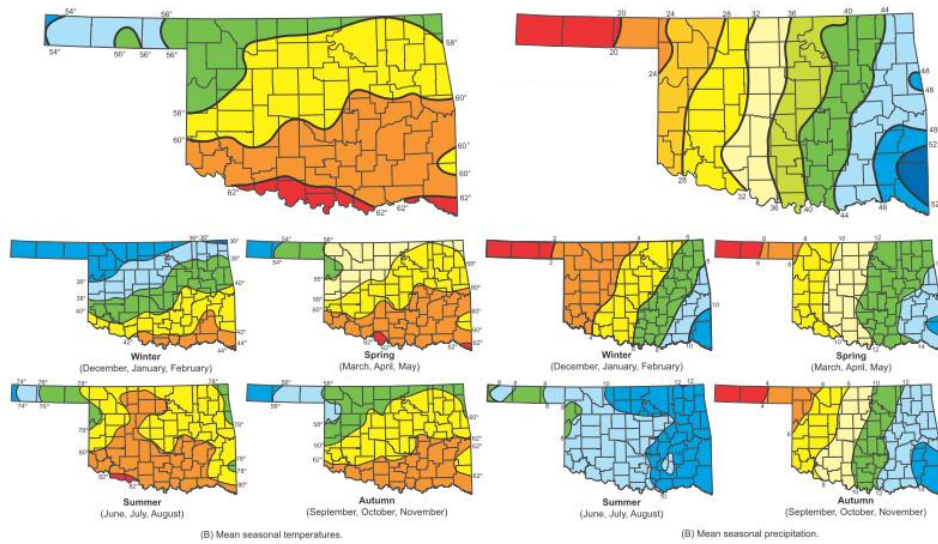


Figure 6 Average Annual Temperature and Average Annual Precipitation of Oklahoma (Keller, 2008)

2.2 Datasets

2.2.1 SMAP Soil Moisture Data

The SMAP baseline science data products (Table 2) are made available publicly through two NASA-designated data centers: the Alaska Satellite Facility (ASF) and the National Snow and Ice Data Center (NSIDC), in Hierarchical Data Format (.h5) with multiple layers. SMAP data used in this study are daily estimates of global land surface conditions in global, cylindrical 36 km Equal-Area Scalable Earth Grid, i.e. L3_SM_P in the table (National Snow and Ice Data Center). Data are available starting April 1st, 2015 and therefore date range for the soil moisture data extends from April 1st, 2015 to July 27th, 2016, over a 16-months period. The unit of remotely sensed SMAP soil moisture measurement is $\text{cm}^3 \cdot \text{cm}^{-3}$.

Table 2 List of SMAP Baseline Science Data Products (from SMAP website)

Product	Description	Gridding (Resolution)	Latency**	
L1A_Radiometer	Radiometer Data in Time-Order	-	12 hrs	Instrument Data
L1A_Radar	Radar Data in Time-Order	-	12 hrs	
L1B_TB	Radiometer T_B in Time-Order	(36×47 km)	12 hrs	
L1B_S0_LoRes	Low-Resolution Radar σ_o in Time-Order	(5×30 km)	12 hrs	
L1C_S0_HiRes	High-Resolution Radar σ_o in Half-Orbits	1 km (1–3 km)#	12 hrs	
L1C_TB	Radiometer T_B in Half-Orbits	36 km	12 hrs	
L2_SM_A	Soil Moisture (Radar)	3 km	24 hrs	Science Data (Half-Orbit)
L2_SM_P*	Soil Moisture (Radiometer)	36 km	24 hrs	
L2_SM_AP*	Soil Moisture (Radar + Radiometer)	9 km	24 hrs	
L3_FT_A*	Freeze/Thaw State (Radar)	3 km	50 hrs	Science Data (Daily Composite)
L3_SM_A	Soil Moisture (Radar)	3 km	50 hrs	
L3_SM_P*	Soil Moisture (Radiometer)	36 km	50 hrs	
L3_SM_AP*	Soil Moisture (Radar + Radiometer)	9 km	50 hrs	
L4_SM	Soil Moisture (Surface and Root Zone)	9 km	7 days	Science Value-Added
L4_C	Carbon Net Ecosystem Exchange (NEE)	9 km	14 days	

2.2.2 Mesonet Ground Observation Data

Mesonet adopts Campbell Scientific 229-L devices due to its ease of use, minimal soil disturbance during installation, small size, ease of automation, and absence of potentially harmful radiation. It measures ΔT , or delta ($^{\circ}\text{C}$), the temperature difference before and after a heat pulse of 50-mA currents is introduced for 21 seconds (Basara and Crawford, 2000). This can be further interpreted into Soil Water Content in the unit of $\text{cm}^3 \cdot \text{cm}^{-3}$ (Illston et al., 2008) using the following formula:

$$WC = WC_r + \frac{WC_S - WC_r}{[1 + (-\alpha \cdot MP)^n]^{(1 - \frac{1}{n})}}$$

where $MP = -c \exp(a\Delta T_{ref})$; WC_S is saturated water content ($\text{cm}^3 \cdot \text{cm}^{-3}$), WC_r is residual water content ($\text{cm}^3 \cdot \text{cm}^{-3}$), MP is soil matrices potential (kPa), ΔT_{ref} is reference temperature differential as stated above, calibration constants $a = 1.788$ ($^{\circ}\text{C}^{-1}$) and $c = 0.717$ (kPa), and empirical constants α (kPa^{-1}) and n (unitless).

Mesonet data are made available publicly through the Oklahoma Climatological Survey. The soil moisture data used in this study are available through the Daily Data Retrieval, where relevant soil moisture data for any time period and any Mesonet station, including soil temperature and soil moisture of 5 cm, 25 cm, 60 cm, and 75 cm depth, are available upon request filling a data retrieval form (Mesonet). Mesonet soil moisture data used in this study in comparison with airborne SMAP data are the top layer data from 5 cm, 25 cm, and 60 cm depth.

2.3 Methods

Various approaches have been adopted to evaluate satellite-based remote sensing soil moisture data versus the in situ observations (Bi et al., 2016; Chen, 2016; Crow et al, 2012; Collow et al., 2012; Draper et al., 2009; Wang et al., 2016; Wu et al., 2016; Zhang et al., 2017). In this study, the spatiotemporal variation pattern of soil moisture in Oklahoma was first mapped and analyzed with the surface soil moisture data from in situ observations. Then the quality of remotely sensed SMAP soil moisture data was assessed in comparison with in situ observations from ground stations of Mesonet, with regards to spatial and temporal variation pattern across the state. As the mismatch of spatial scale exists between grid-based satellite retrievals and point-based in situ observations, remotely sensed SMAP data was downscaled, and point-based Mesonet data was spatially interpolated, to make the comparison valid and accurate (Mohanty and Skaggs, 2001).

2.3.1 Spatial Downscaling Method for Remotely Sensed SMAP Data

The spatial resolution for retrieved SMAP Passive data is 36 kilometers by 36 kilometers, which is too coarse for comparison with point-based Mesonet data. Thereby spatial downscaling of the remotely sensed data is necessary. Nearest neighbor resampling method is applied to downscale the soil moisture data into the spatial resolution of 25 kilometers, in order to be consistent with other remote sensors including AMSR-2. Spatial reference for all data have been transferred into Universal Transverse Mercator (UTM) World Geodetic System 1984 (WGS84) coordinates (Wang et al., 2008).

2.3.2 Spatial Interpolation Method for Point-based Mesonet Data

Soil composition, vegetation, topography, hydrological process, and human activity including tillage, cropping, and irrigation all contribute to the spatiotemporal heterogeneity of soil water content. Understanding the spatial and temporal variability of soil moisture is essential in predicting land surface processes (Miralles et al., 2010). With the need to input spatially and temporally varying soil moisture to hydrological and meteorological models, the understanding of variability of soil properties and the demand for interpreting variability have accelerated (Yao et al., 2013). Kriging is a common geostatistical technique for interpolation that considers not only the autocorrelation based on distance but also the semi-variance quantifying spatial dependence (Yuan et al., 2017). It has proven to produce the optimum linear unbiased estimate (Pandey et al., 2010).

2.3.3 Evaluation of Remotely Sensed SMAP Data with *in situ* Mesonet Observations

Four statistics were used to evaluate the performance of SMAP L3 soil moisture product, including Coefficient of Determination (R^2 or R squared), Mean Difference (MD), Mean Absolute Error (MAE), Root Mean Squared Error (RMSE). Since the remote sensors measures the reflected surface thermal energy emission, the comparisons were mainly made between SMAP Passive data versus Mesonet surface soil moisture at the top 5 centimeters, only with SMAP-Mesonet correlations studied with Squared Pearson Correlation Coefficient or R^2 at 5, 25, and 60 centimeters depth to make the evaluation more comprehensive.

Squared Pearson Correlation Coefficient, or R^2 , measures the proportion of the variance in the satellite soil moisture retrievals attributable to the variance in *in situ* soil moisture measurements. R^2 can be calculated as:

$$R^2 = \frac{\sum_{i=1}^N (y_i - \bar{y}_i)(\hat{y}_i - \bar{\hat{y}}_i)}{\sqrt{\sum_{i=1}^N (y_i - \bar{y}_i)^2 \sum_{i=1}^N (\hat{y}_i - \bar{\hat{y}}_i)^2}}$$

where \bar{y} represents the mean value of satellite retrievals ($\text{cm}^3 \cdot \text{cm}^{-3}$), and \hat{y} is the *in situ* measurements ($\text{cm}^3 \cdot \text{cm}^{-3}$).

The MD, also called bias, represents the systematic difference between satellite and *in situ* data, and can be calculated using the following formula:

$$MD = \frac{\sum_{i=1}^N (y_i - \hat{y}_i)}{N}$$

The MAE measures the average magnitude of the difference between satellite and *in situ* data, without considering their direction. The MAE is calculated as:

$$MAE = \frac{\sum_{i=1}^N |y_i - \hat{y}_i|}{N}$$

The RMSE measures the absolute difference between SMAP L3 soil moisture retrievals relative to the Mesonet soil moisture observations. The RMSE is calculated using the formula:

$$RMSE = \sqrt{\frac{\sum_{i=1}^N (y_i - \hat{y}_i)^2}{N}}$$

When comparing the variation of MD and RMSE, both statistical metrics are divided by the mean of the referenced observation value, in this case the mean of \hat{y} , or the average of the in situ measurements, to calculate Relative MD (RMD) and Relative RMSE (RRMSE), respectively, in comparison to the size of mean. RRMSE represents percentage variation in accuracy. The two parameters bear the unit of percent (%), and are denoted and calculated as follows:

$$RMD = \frac{MD}{\bar{\hat{y}}_i} = \frac{\frac{\sum_{i=1}^N (y_i - \hat{y}_i)}{N}}{\frac{\sum_{i=1}^N \hat{y}_i}{N}}$$

$$RRMSE = \frac{RMSE}{\bar{\hat{y}}_i} = \frac{\sqrt{\frac{\sum_{i=1}^N (y_i - \hat{y}_i)^2}{N}}}{\frac{\sum_{i=1}^N \hat{y}_i}{N}}$$

2.3.4 Spatial Variation Pattern: Precipitation, Temperature, and Climatic Inference

Spatial variation patterns of Oklahoma soil moisture is evaluated based on the climatic conditions, along the average annual precipitation and temperature gradient.

As is stated in section 2.1.2, the average annual precipitation ranges from 56 inches (1422 mm) in the southeast to 17 inches (431 mm) in the far western panhandle. Based on this empirical information during 1961 – 1990 derived from PRISM model

(USDA-NRCS), the state of Oklahoma is classified into three precipitation zones (Figure 7): 1. Arid Zone in the west with average annual precipitation lower than 28 inches (711 mm), 2. Semi-arid Zone in the center with precipitation higher than 28 inches and lower than 40 inches (1016 mm), 3. Wet Zone in the east with precipitation higher than 40 inches.

Oklahoma Precipitation Zones

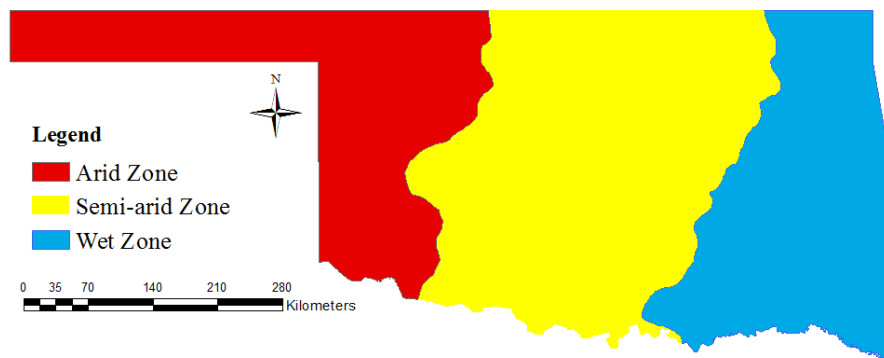


Figure 7 Oklahoma Precipitation Zones

The average annual temperature decreases from 62 °F (17 °C) along the Red River on the southern border to 58 °F (14 °C) along the northern border, and further decreases to 54 °F (12 °C) on the tip of panhandle. Therefore, the state of Oklahoma is divided into three temperature zones (Figure 8): 1. Cool Zone in the northwest which covers the panhandle area with average annual temperature lower than 58 °F (14 °C), 2. Mild Zone in the center with temperature higher than 58 °F and lower than 60°F (16 °C), 3. Warm Zone in the southeast with temperature higher than 60°F.

Oklahoma Temperature Zones

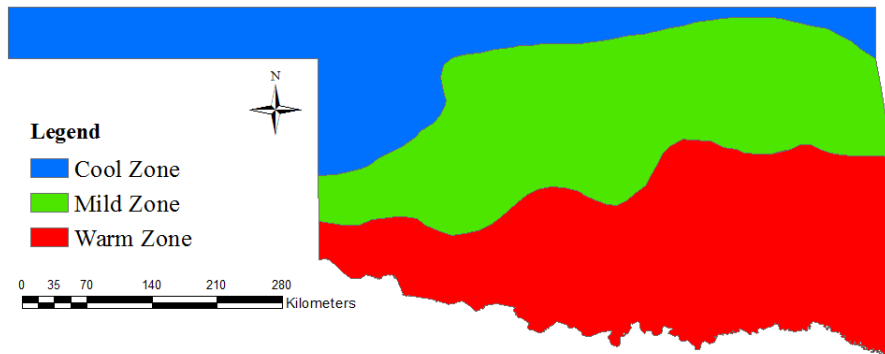


Figure 8 Oklahoma Temperature Zones

On the basis of precipitation and temperature zoning schemes stated above, the state of Oklahoma can be further classified into nine climate divisions, which coincides with Guttman and Quayle (1996)'s Climate Divisions scheme that compiled 344 divisions for 48 contiguous U.S. states based on year-monthly means of water-equivalent precipitation and temperature since 1895 (OCS, 2016). The climate divisions, unlike precipitation and temperature zones whose borders are based on natural conditions, draw boundaries on the basis of county. The nine Oklahoman climate divisions overlap three precipitation zones in the East-West direction and three temperature zones in the North-South direction, and they include: 1. Panhandle, 2. North Central, 3. Northeast, 4. West Central, 5. Central, 6. East Central, 7. Southwest, 8. South Central, and 9. Southeast.

Oklahoma Climate Divisions

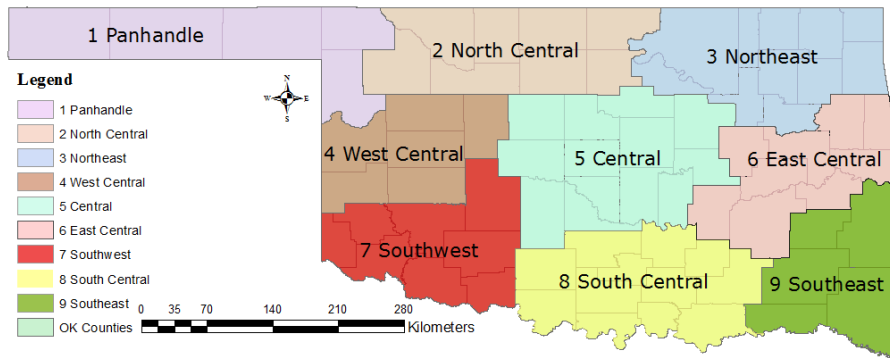


Figure 9 Oklahoma Climate Divisions

Data are analyzed based on for both state-as-a-whole and each of the divisions (zones), observing the spatial (geographical) variation patterns and temporal (seasonal) variability patterns, and examining the SMAP-Mesonet correlation with statistics including R^2 , MD, MAE, and RMSE, with the average monthly soil moisture data.

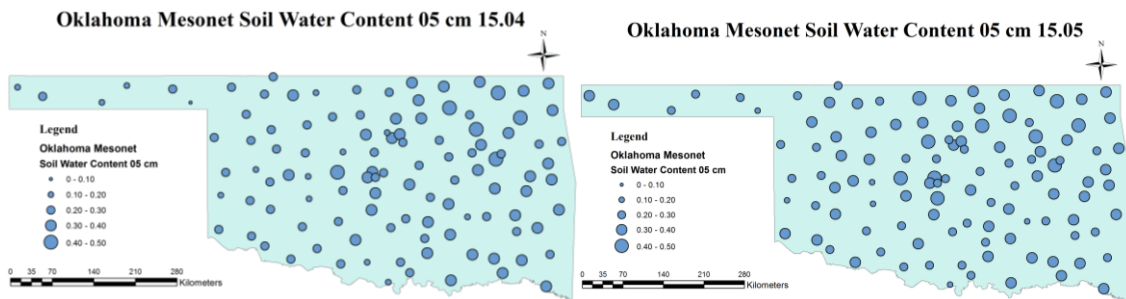
2.3.5 Temporal Variation Pattern: Seasonal Variability

Temporal Variation Pattern of Oklahoma soil moisture is assessed on the basis of both monthly average variation pattern and seasonal variability. As the state of Oklahoma entirely lies in the Northern hemisphere, the each of the four astronomical seasons are defined and counted for the months as follows: 1. Spring - March Equinox to June Solstice, April to June; 2. Summer - June Solstice to September Equinox, July to September; 3. Fall (autumn) - September Equinox to December Solstice, October to December; and 4. Winter - December Solstice to March Equinox, January to March. This seasonal classification scheme was intentionally made to incorporate months with frequent thunderstorms and tornadoes during April to June, in order to further determine the impact of extreme weather events on the efficiency of remotely sensed data.

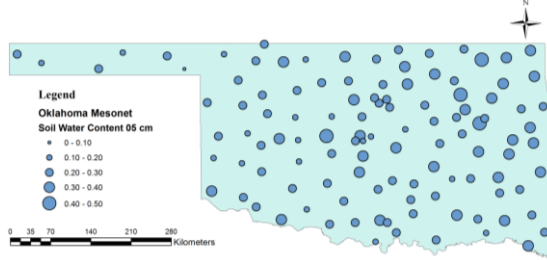
Chapter 3. Comparison of SMAP Passive and Mesonet Soil Moisture

3.1 Spatial Variation in Oklahoma Soil Moisture based on Mesonet Data

Average monthly surface soil moisture derived from Mesonet at top 5 cm was plotted using graduated symbols to show the quantitative difference in in situ soil moisture observations at each station (Figure 10). The station-wise monthly data ranged from 0.045 ($\text{cm}^3 \cdot \text{cm}^{-3}$) in September 2015 to 0.459 ($\text{cm}^3 \cdot \text{cm}^{-3}$) in May 2015. The lowest soil moisture value averaged 0.086 ($\text{cm}^3 \cdot \text{cm}^{-3}$) whilst maximum was 0.4332 ($\text{cm}^3 \cdot \text{cm}^{-3}$) for the 16 month period. The point plots showed a constantly high soil moisture value ($\geq 0.25 \text{ cm}^3 \cdot \text{cm}^{-3}$) in the northeastern portion of the state, remarkably in the Ozark mountain range and Cherokee Platform where vegetation is relatively dense with forest ranges. The lowest soil moisture value typically occurs in the eastern half of the panhandle. From the temporal perspective, summer (July to September) months observe less high soil moisture values, which mostly concentrates within the northeastern Oklahoma, and more low soil moisture values, which may attribute to low precipitation (Miller and Fox, 2017) and high evapotranspiration rate due to the high temperature (Jin and Mullens, 2014).



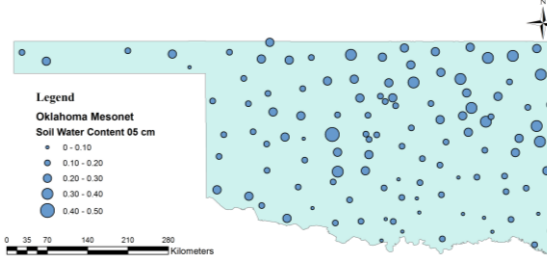
Oklahoma Mesonet Soil Water Content 05 cm 15.06



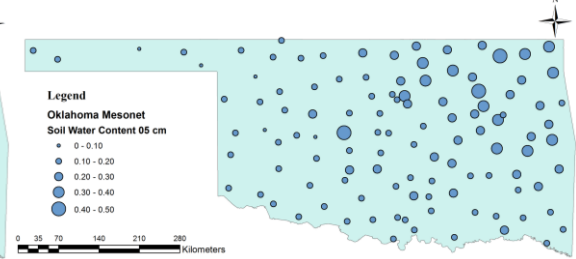
Oklahoma Mesonet Soil Water Content 05 cm 15.07



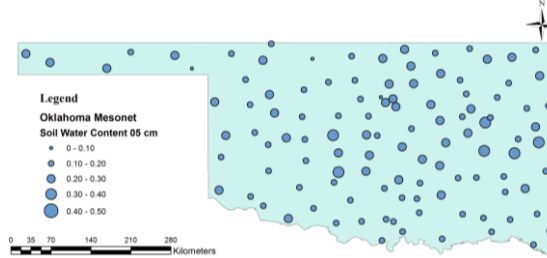
Oklahoma Mesonet Soil Water Content 05 cm 15.08



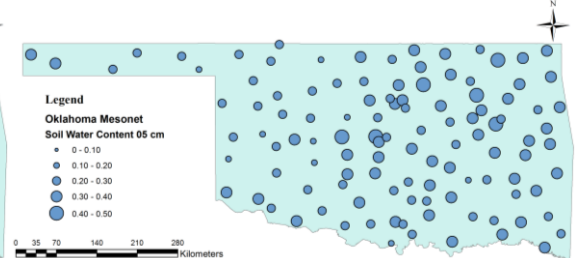
Oklahoma Mesonet Soil Water Content 05 cm 15.09



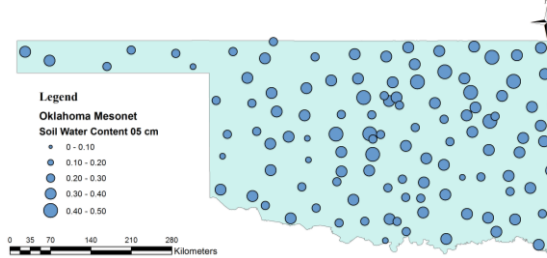
Oklahoma Mesonet Soil Water Content 05 cm 15.10



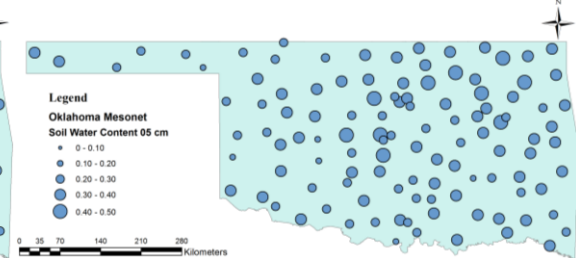
Oklahoma Mesonet Soil Water Content 05 cm 15.11



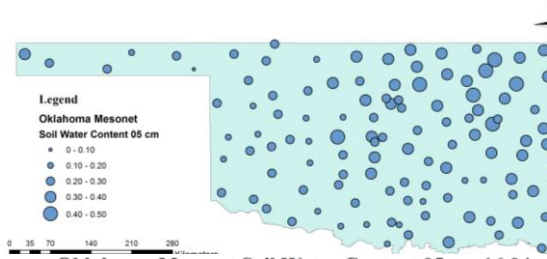
Oklahoma Mesonet Soil Water Content 05 cm 15.12



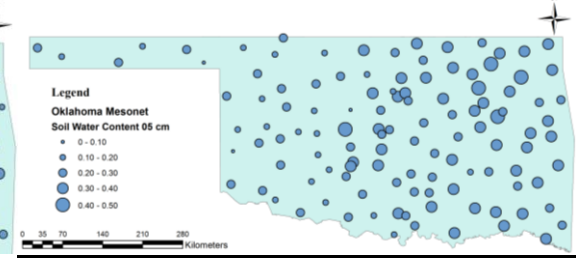
Oklahoma Mesonet Soil Water Content 05 cm 16.01



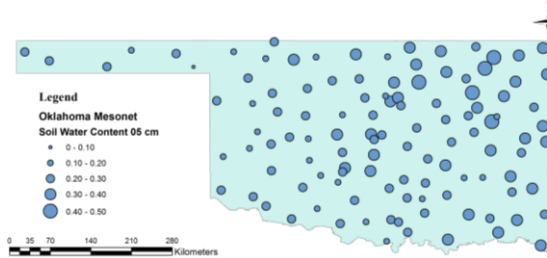
Oklahoma Mesonet Soil Water Content 05 cm 16.02



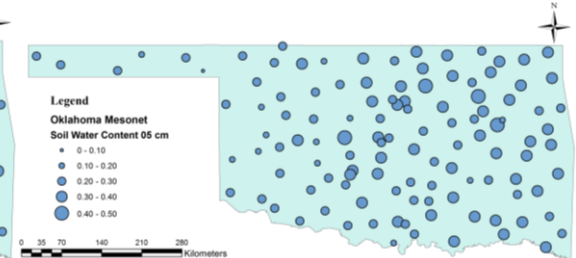
Oklahoma Mesonet Soil Water Content 05 cm 16.03



Oklahoma Mesonet Soil Water Content 05 cm 16.04



Oklahoma Mesonet Soil Water Content 05 cm 16.05



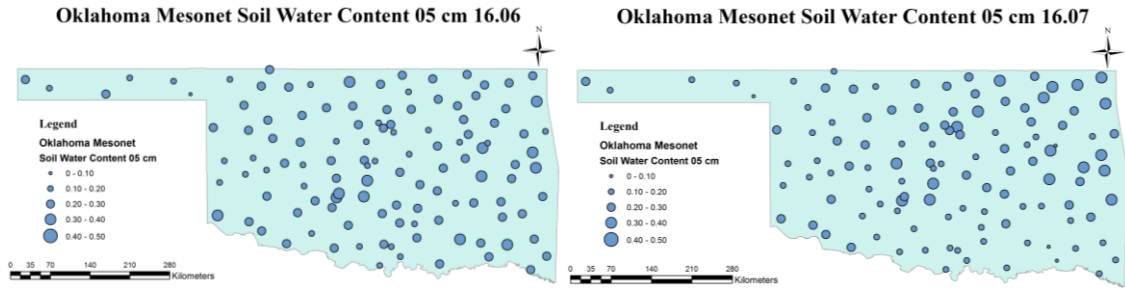


Figure 10 Average Monthly Surface Soil Moisture (Mesonet, top 5 cm)

In order to quantify the spatial variation pattern of soil moisture value, distribution of 16-month-average Mesonet surface soil moisture was plotted along the longitudinal and latitudinal gradient respectively. Results show an observable trend for higher soil moisture value both in the eastern and southern directions. The longitudinal distribution verifies the spatial observation that the highest soil moisture value occurs in the far east, whereas the lowest in the eastern half of the panhandle region. The lowest soil moisture value increased from lower than 0.1 ($\text{cm}^3 \cdot \text{cm}^{-3}$) to higher than 0.15 ($\text{cm}^3 \cdot \text{cm}^{-3}$) both from west to east and from south to north, while the highest soil moisture value from lower than 0.25 ($\text{cm}^3 \cdot \text{cm}^{-3}$) to nearly 0.3 ($\text{cm}^3 \cdot \text{cm}^{-3}$) for both directions.

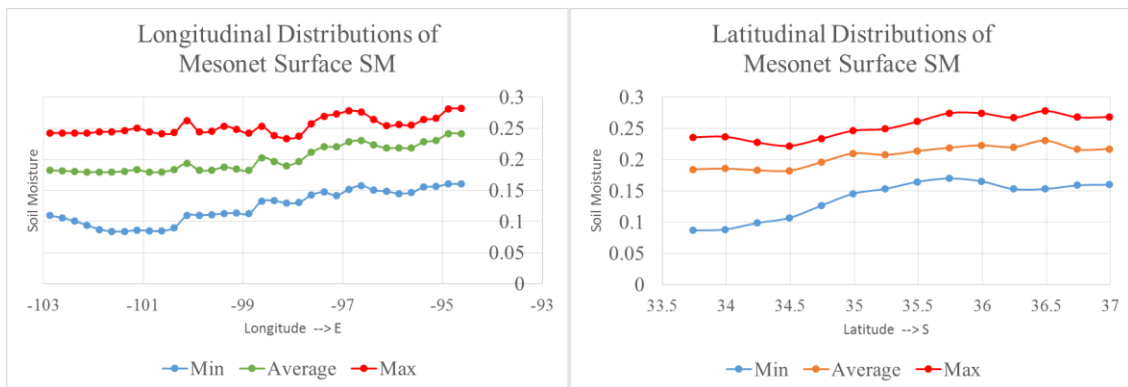
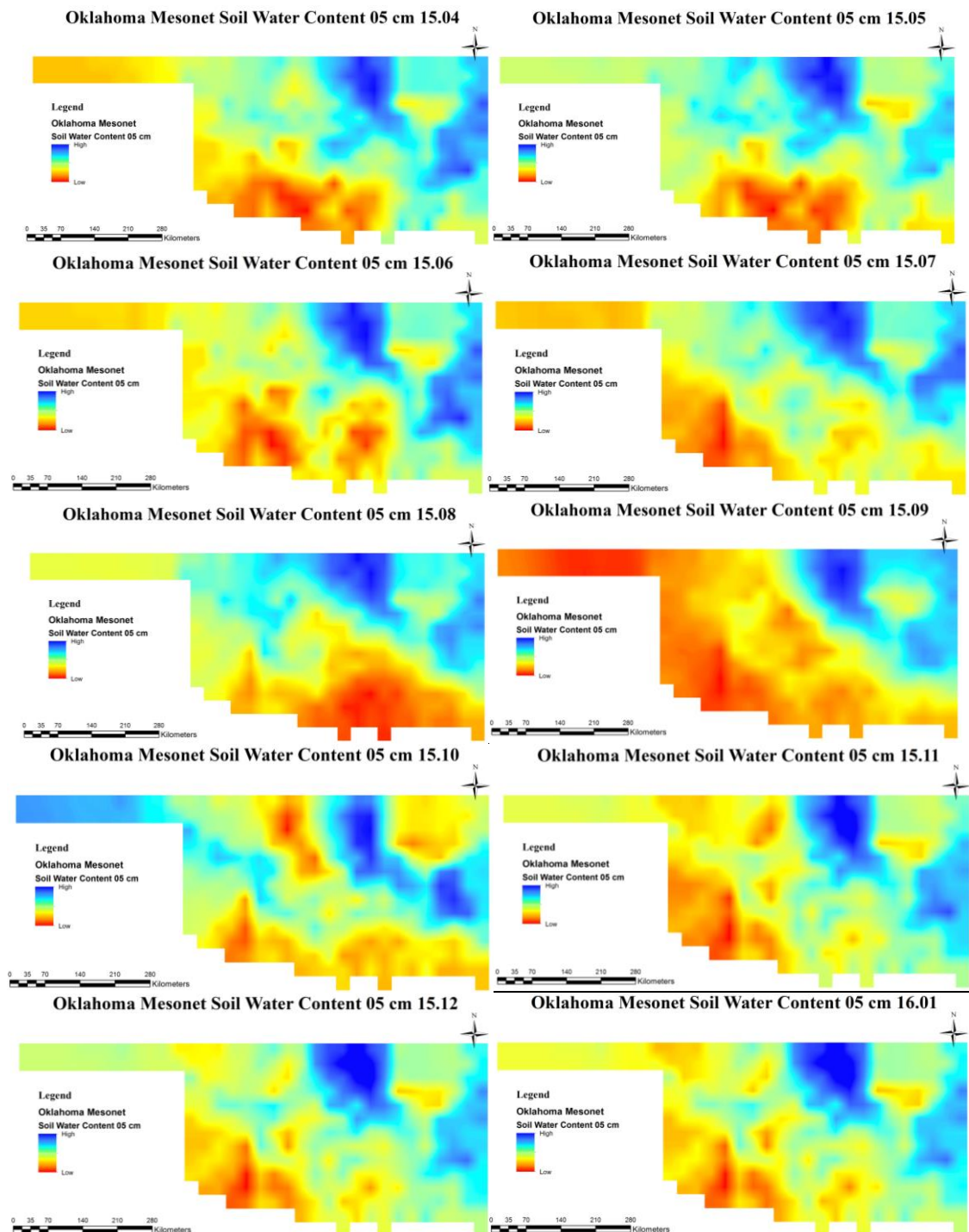


Figure 11 Longitudinal and Latitudinal Distributions of Mesonet Surface SM

The point-based in situ observation data were spatially interpolated to make the soil moisture value continuous all over the state, to inspect the monthly spatial variation pattern, and to upscale the datasets into grid-based in order to be comparable with the grid-based satellite retrievals.



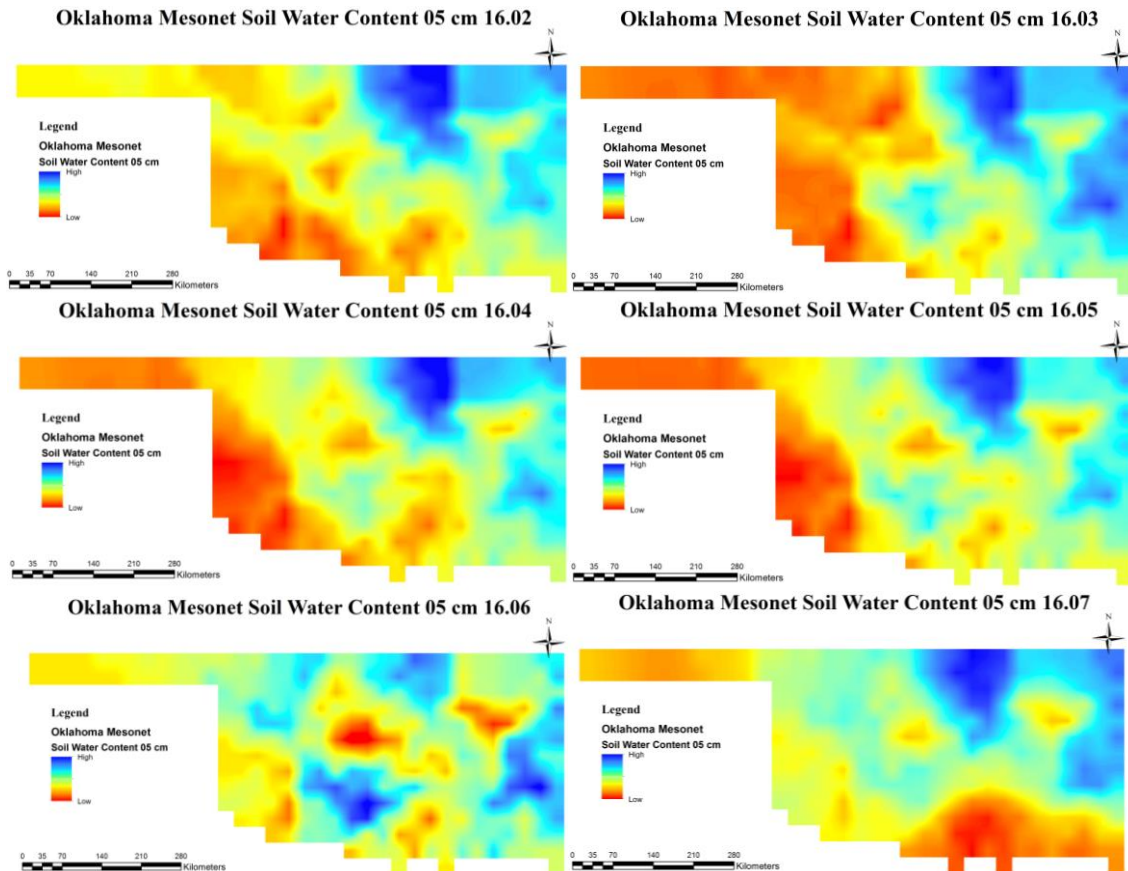


Figure 12 Spatially Interpolated Mesonet Average Monthly Surface Soil Moisture

The pattern of soil moisture distribution can be easily observed and summarized as soil moisture content gradually increasing from southwest to northeast, with highest value in the Ozark mountain ranges and Cherokee Platform on the upper right corner and lowest along eastern panhandle – southern border. As is stated above, this may be mainly caused by meteorological factors such as precipitation and temperature which impacts the hydrological process of evapotranspiration. Other factors such as soil texture and vegetation type, topography and elevation, may also contribute to the capacity of water to remain in the soil pores. On the other hand, soil water content may have strong implication for Earth surface physiographic factors and hydrometeorological processes.

3.2 Temporal Variation in Oklahoma Soil Moisture

Time series analysis were performed for average monthly soil moisture data from both in situ observations of Mesonet and remotely sensed SMAP retrievals with precipitation and temperature information retrieved from Mesonet, to examine the seasonal variability of each factor and interaction of precipitation and temperature versus soil water content.

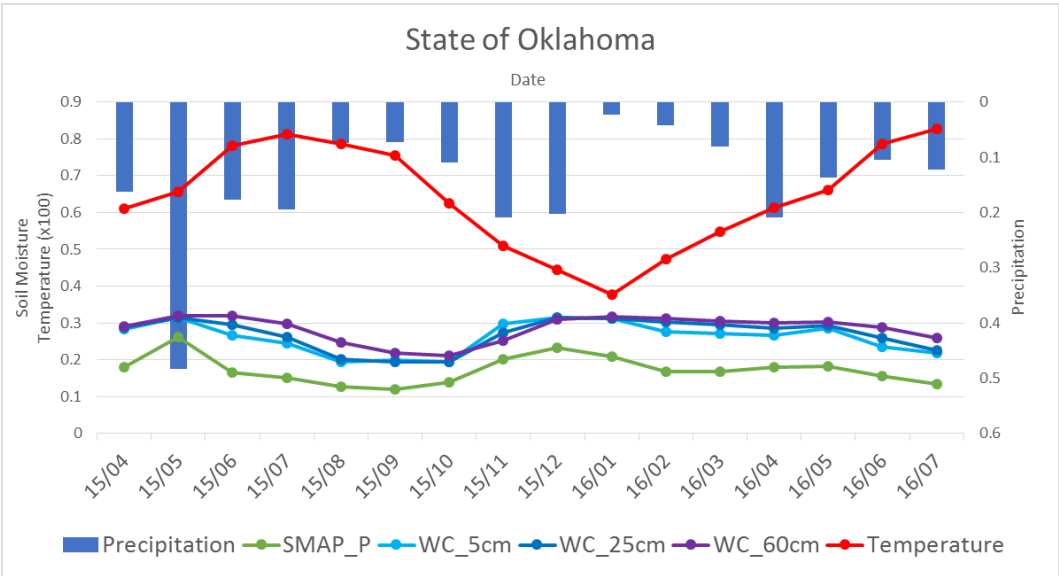


Figure 13 Time Series Analysis of Soil Moisture as a Function of Precipitation and Temperature for State-as-a-Whole

The soil water contents for both SMAP retrieval and Mesonet observations bear the unit of $\text{cm}^3 \cdot \text{cm}^{-3}$, as is described in section 2.2. Precipitation represents daily rainfall with the unit of inch (in), while temperature stands for average daily air temperature with the unit of Fahrenheit degrees ($^{\circ}\text{F}$), whose value is divided by 100 in order to fit to the y-axis with soil water content numbers. The numbers are denoted for soil water content and temperature on the left axis, whilst precipitation on the right.

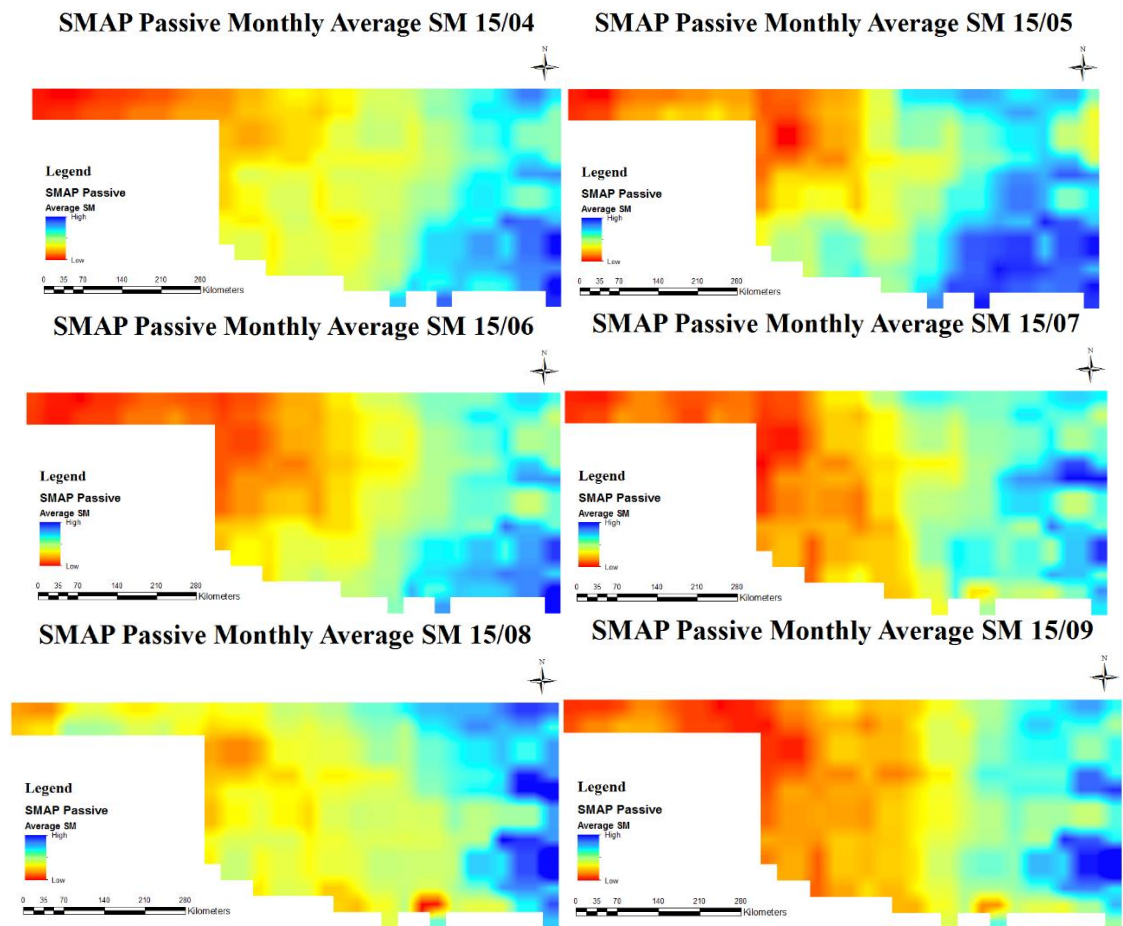
Generally, soil moisture, precipitation and temperature all follow a regular variation pattern of seasonal fluctuation. During winter time, even with lowest precipitation, evapotranspiration process is slow due to low temperature, so that soil water content may keep at a relatively high status. This is even more applicable to vadose zone (25 cm and 60 cm) than surface (5 cm) soil moisture. Then the amount of soil water decreases as the temperature rises, but due to the increasing precipitation, the decrease in soil moisture is low. Tornadoes hit Oklahoma during the months of April and May, when soil water content experiences a rapid increase in response to extensive precipitation and slowdown of temperature increase rate, as a result of frequent thunderstorms. Temperature keeps increasing until mid-summer causing escalating evapotranspiration rate, by which soil water content is withdrawn progressively, altogether with low precipitation during summer months. Subsequently with the cooling off and rising rainfall during fall, soil water repository gets filled up and reaches its peak again. Therefore it is not too much to say that fluctuation of soil moisture is a function of variation in precipitation and temperature.

Other than soil moisture – precipitation – temperature interactions, Figure 13 also explains SMAP – Mesonet soil moisture data correlations. SMAP follows identical seasonal variation pattern with Mesonet – seasonal fluctuation with high level in winter and tornado season and low in summer – which indicates a high correlation between the two datasets, which will be analyzed in the subsequent chapters. In addition, the sharper peak of SMAP than Mesonet data for May 2015 implies that SMAP may be more sensitive to abrupt weather condition such as thunderstorm than Mesonet. Spatiotemporal SMAP – Mesonet correlation is analyzed in the next two chapters.

Chapter 4. Spatial Analysis of the SMAP Soil Moisture Comparing to the Mesonet Observations

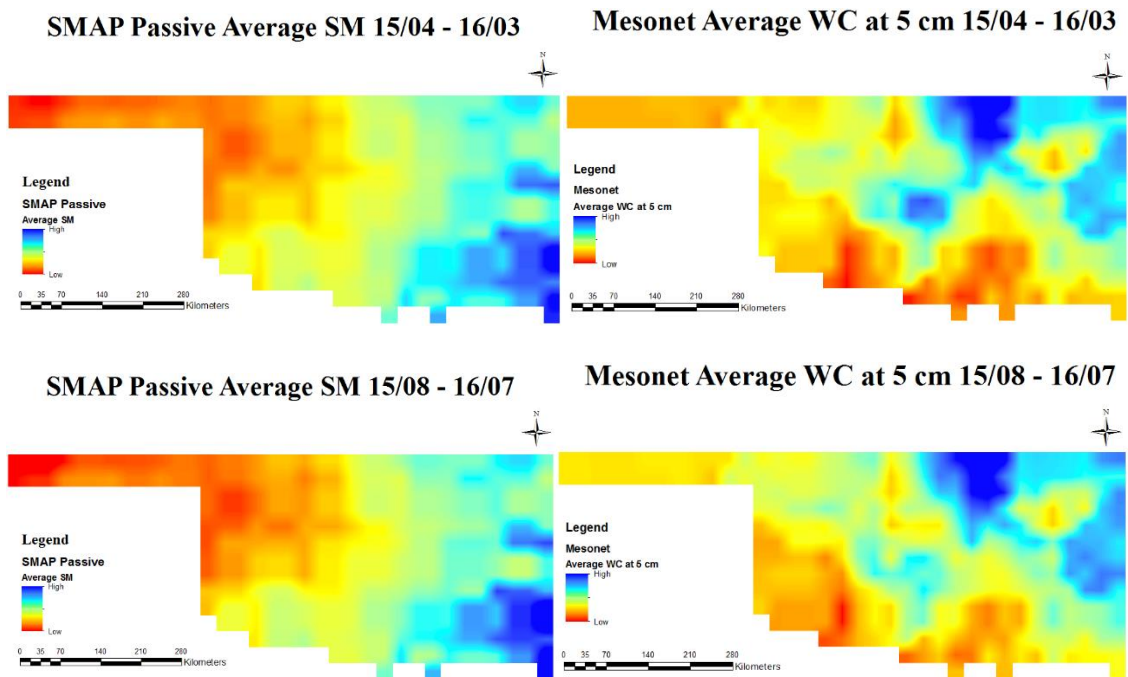
4.1 Statewide Comparison of SMAP and Mesonet Soil Moisture

As is described in the methodology section of Chapter 2, gridded remotely sensed SMAP data was downsampled from 36 km spatial resolution to 25 km using the nearest neighbor resampling scheme. Thus far, the downscaling of SMAP data and spatial interpolation of Mesonet information have matched the spatial resolutions of remote sensor retrievals and in situ observations and therefore the two datasets are comparable on the grid-basis.



The spatial distribution pattern of SMAP soil moisture retrievals (Figure 14) share similarities but also differs from the Mesonet observations (Figure 12). Both show high soil water content in the eastern portion of the state, and low in the west. But the spatial gradient for SMAP lies on northwest – southeast direction, whereas Mesonet on southwest – northeast direction. For SMAP retrievals, the lowest soil water content is found on the western tip of the panhandle and the highest in the Ouchita mountain range on the lower right corner.

To verify this trend, the grid-based average of soil water content for the first 12 months (April 2015 through March 2016), the last 12 months (August 2015 through July 2016), and the entire 16 month (April 2015 through July 2016) for both SMAP retrievals and Mesonet observations were calculated and mapped (Figure 15) to further analyze the spatial distribution patterns of soil moisture.



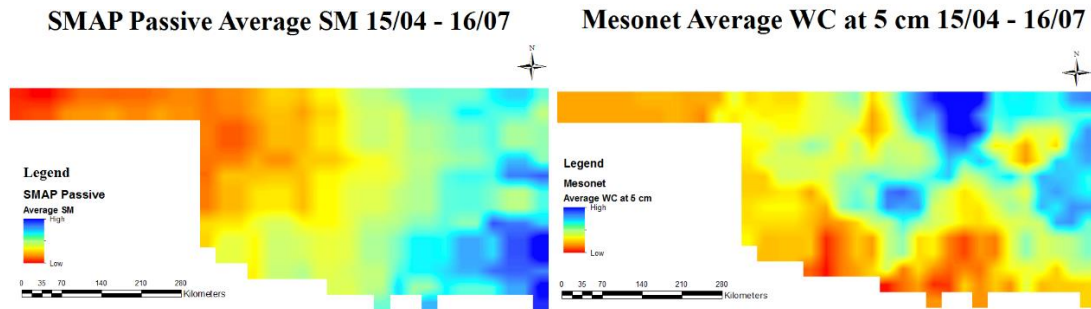


Figure 15 Statewide SMAP versus Mesonet Average Monthly Surface Soil Moisture for the First 12 Months, the Last 12 Months, and the Entire 16 Month

The annual and 16-months averages demonstrated the same geographical gradient of soil moisture with the monthly data, i.e. lies on northwest – southeast direction for SMAP, and southwest – northeast direction for Mesonet. More can be noticed by comparing the first and last 12-months averages. According to SMAP retrievals, the first 12 months is relatively wetter than the last 12 months. This is possibly due to the extensive precipitation events during April to July 2015, especially in May, which is discovered from the time series analysis in Figure 13 of Section 3.2. The same time period of 2016 had far less precipitation, making the annual average soil water repository overall lower than the preceding year statewide. The Mesonet data reveal that the higher soil moisture for April to July 2015 is mainly observed in central Oklahoma within the area so-called *tornado alley*. The soil water retention in this region can be mainly attributable to three factors: (1) high precipitation due to thunderstorms and tornadoes, (2) sedimentary geology which impedes groundwater flow, and (3) land use and land cover change in the Oklahoma City metropolitan area due to extensive human activity, such as paving cement and concrete roads retards surface runoff and increases local infiltration.

In order to quantify the SMAP – Mesonet correlation and to test the degree of similarities and differences, the four statistical metrics including Pearson’s R^2 , MD, MAE, and RMSE (Section 2.3.3) were carried out for each of the 25 km grids, and visualized for spatial pattern of SMAP versus Mesonet correlations.

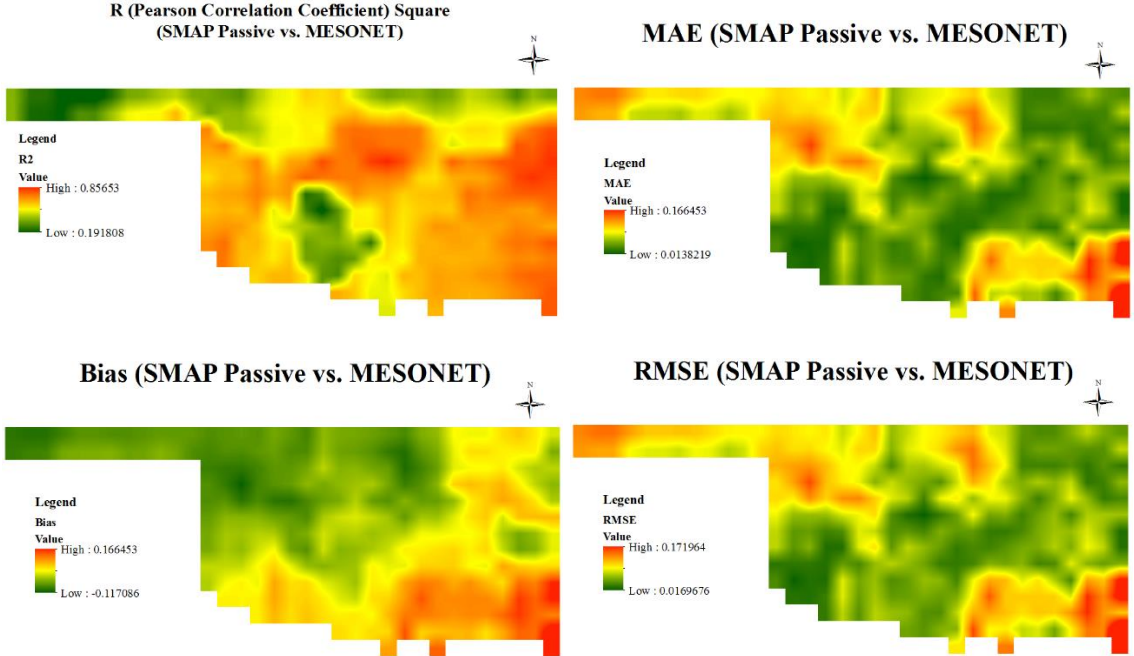


Figure 16 Statistics for SMAP – Mesonet Correlation Statewide

Overall SMAP soil moisture retrievals has shown a relatively high correlation (denoted red in Pearson’s R^2 plot) and a low error (denoted green in MD, MAE, and RMSE plots) with Mesonet observations, with remarkably high R^2 and low error in the central zone. The western tip of the panhandle region and the southeastern corner of the state have shown a relatively low correlation and high error, indicating a deviation between remote sensing retrievals and in situ observations at the top-left and bottom-right areas. This may due to the frequent variation in soil water content as a result of widely fluctuating precipitation and temperature within these areas.

4.2 Evaluation of SMAP based on Climatic Conditions

The spatial variation patterns of SMAP–Mesonet correlations are further studied in terms of climatic conditions based on average annual precipitation and temperature distributions, by dividing the state of Oklahoma into three precipitation zones, three temperature zones, and nine climatic regions as a combination of precipitation and temperature effects. Time series analysis of seasonal variability, exploratory data analysis with box-and-whisker plots, and SMAP Soil Moisture product performance evaluation with the four statistical metrics were performed for each climatological region.

4.2.1 SMAP Evaluation based on Precipitation Zones

Descriptive and statistical analyses were made within the three precipitation zones in Oklahoma, with two borders drawn on lines of 28-inches' and 40-inches' average annual precipitation, respectively (Figure 7).

Time series analyses were first performed to qualitatively examine the seasonal variation patterns of soil water content and SMAP performance within each precipitation zone. Precipitation and temperature information were retrieved from the Mesonet observations and averaged into monthly values.

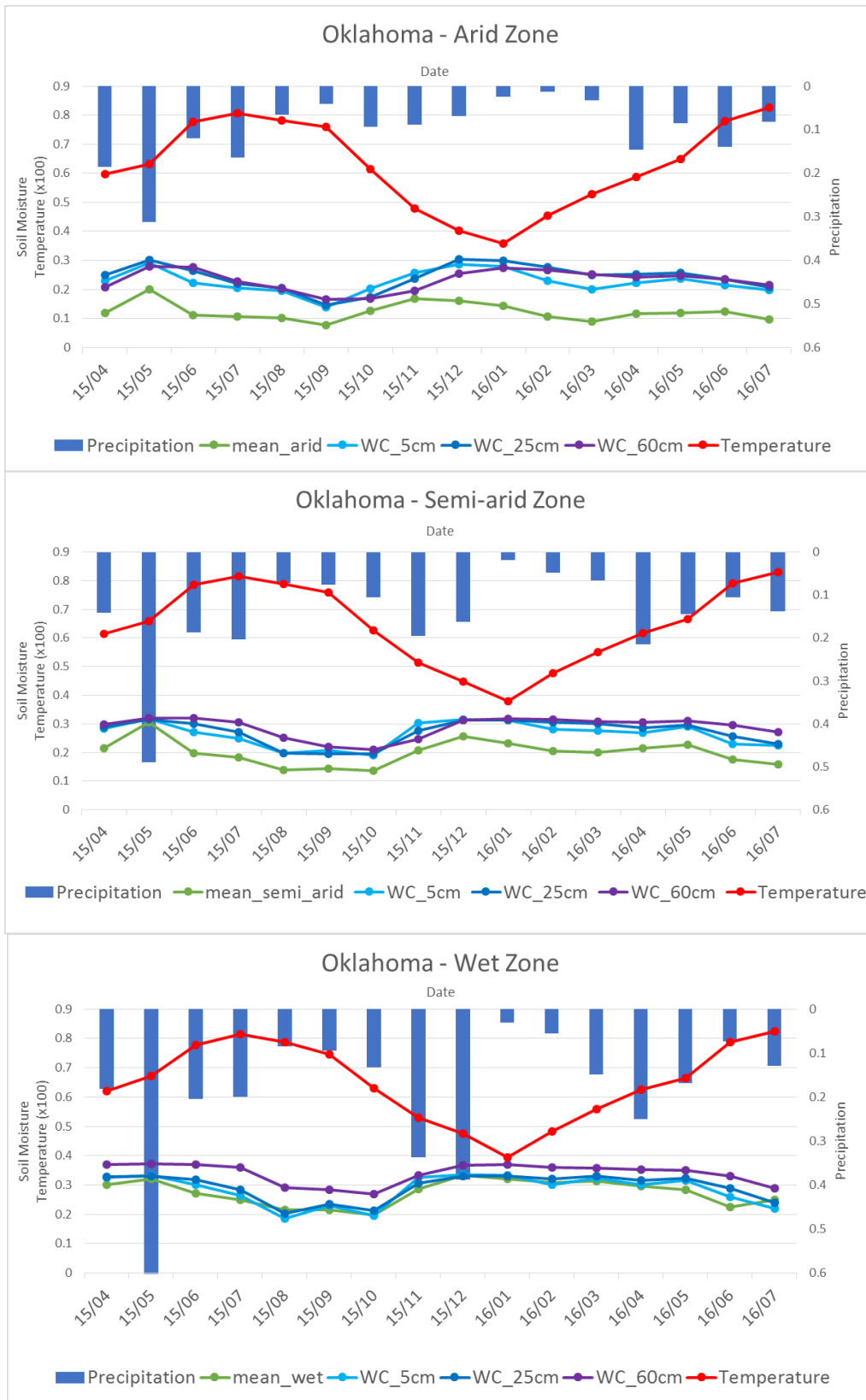


Figure 17 Time Series Analysis of Soil Moisture based on Precipitation Zones

Results show a regular seasonal fluctuation and interrelations of soil water content, precipitation, and temperature. As stated in Section 3.2, precipitation values doubled and, in some months, even tripled from arid to wet zone, whereas temperature remained almost the same in the East – West direction. As for soil water content, surface moisture increased, but very little, whilst the root zone moisture increased noticeably, as much as 150 to 200 %, according to Mesonet observations. The SMAP values, which presumably measure the surface water content, have actually responded with deep-layer moisture, increasing at a similar rate from west to east, but followed a closer seasonal variation pattern with top-layer within each precipitation zone. Overall SMAP retrievals follow the same seasonal variation pattern with Mesonet observations, but underestimate soil water content than Mesonet, with exceptions in wet zone during summers, which is observed for the months of August 2015 and July 2016. The changes in precipitation and temperature are more likely to exert a more significant and immediate effect on surface than root zone water content. This is even more obvious in the wet zone than the arid zone for the decrease in precipitation, as is observed for the sharper decline of surface soil moisture in August 2015, on the other hand more evident in the arid zone than the wet zone for sudden increase of rainfall, such as May 2015.

Then the box-and-whisker diagram is plotted to visualize variation in descriptive statistics including minimum, mean, median, maximum, outliers, as well as lower and upper quartiles values among the different zones.

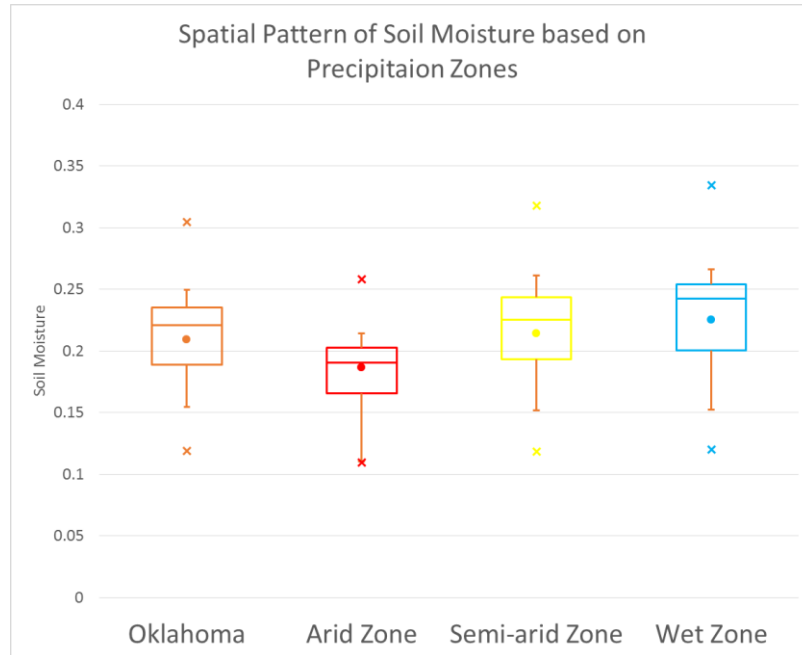


Figure 18 Box-and-Whisker Diagram for Each Precipitation Zone

The top and bottom boundary of the box shows the upper and lower quartiles, whereas the line in the box represents median and the dot for mean value. The whiskers illustrate the spread of all of the data, whose top and bottom indicate the maximum and minimum values. The crosses represent the outliers, which is 1.5 times more than the upper quartile, or 1.5 times less than the lower quartile. The colors in each box are matched to the corresponding precipitation zones with the same colors in Figure 7. Based on this knowledge, the mean, median, and overall quantitative distributions of the soil water content are observed to increase, also the data ranges to expand, from the arid zone to the wet zone, or from the west to the east, which is 20% higher in the semi-arid zone and 30% higher in the wet zone than the arid zone. Wet zone has the widest data range, but in general variation within each precipitation zone is small, which is less than $0.06 \text{ cm}^3 \cdot \text{cm}^{-3}$. This is obvious as the more rainfall, the more infiltration, and certainly the higher soil water content observed.

To further quantitatively measure the variations, statistics including Pearson's R^2 , MD, MAE, and RMSE, as well as the relative RMD and RMSE, or RMD and RRMSE, were calculated for each precipitation zone and plotted as follows:

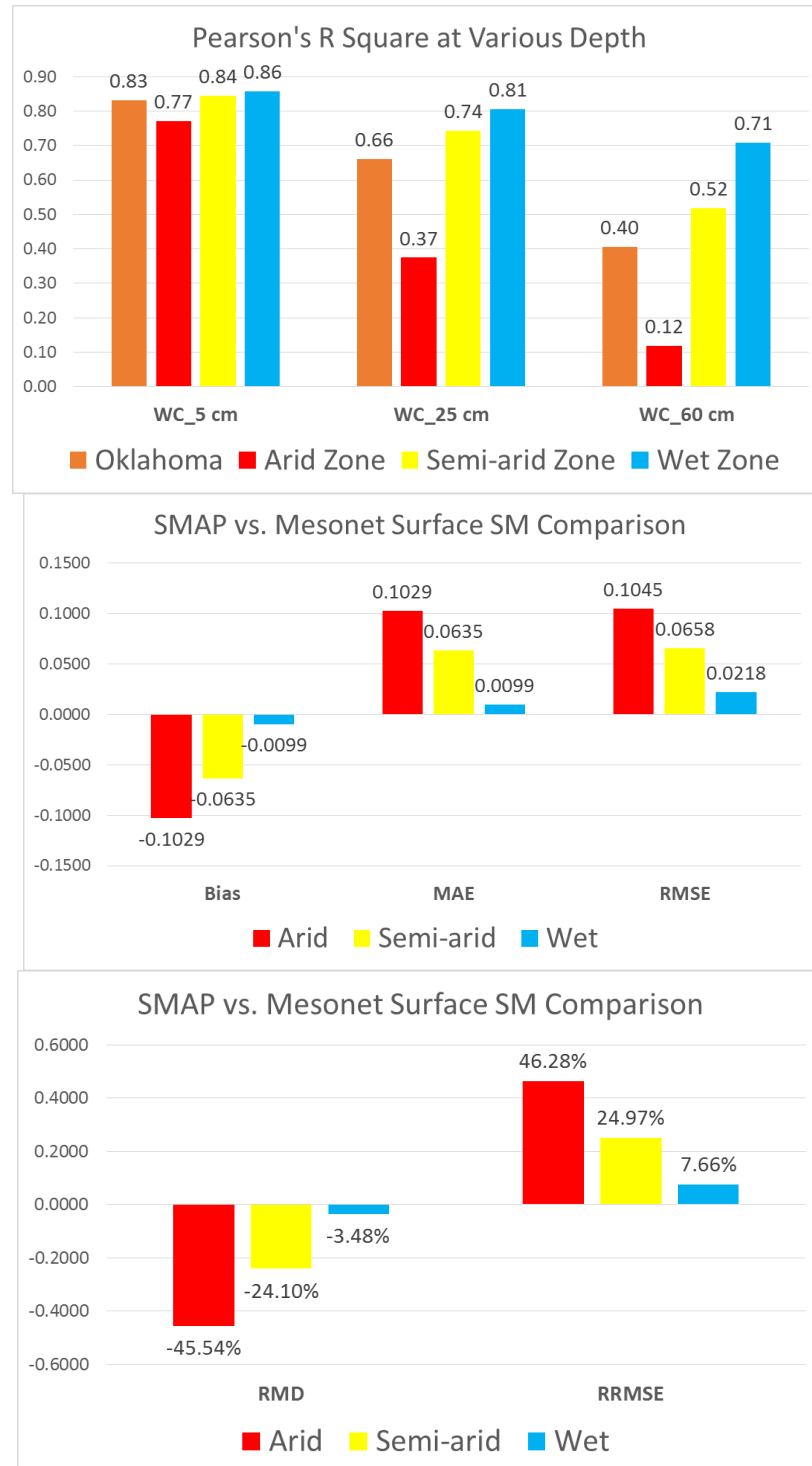
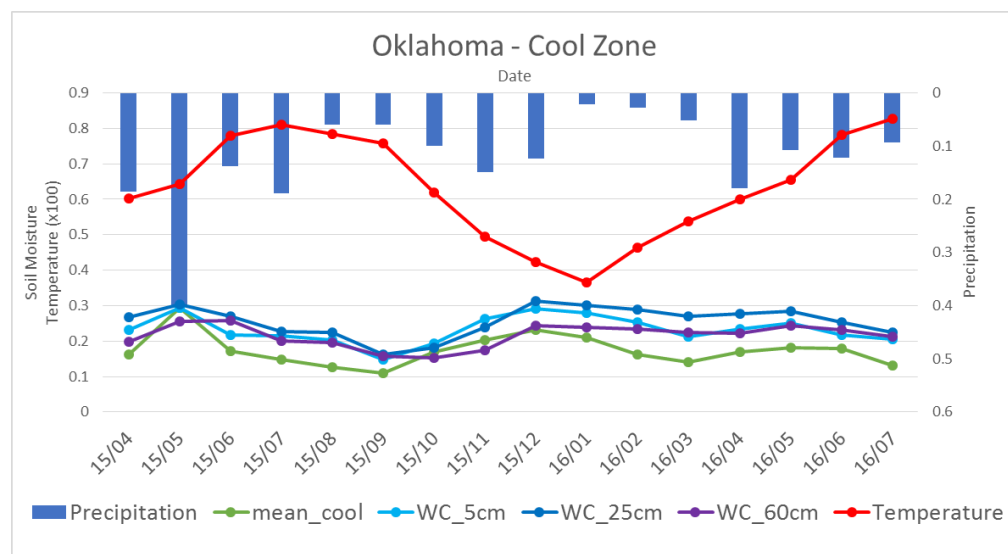


Figure 19 Statistics of SMAP – Mesonet Correlation for Each Precipitation Zone

All the statistical metrics have shown an apparent trend of higher correlation and lower error between SMAP retrievals and Mesonet observations for the wet zone than the arid zone, and remarkably strong association for surface soil water content with all R^2 values greater than 0.75. Deviation is high for root zone soil moisture measurements in the arid zone. The negative values of MD, or bias explains the underestimation of SMAP soil moisture retrievals than in situ Mesonet observations. The RRMSE demonstrates that the error shrinks to half from the arid zone to the semi-arid zone, and decreases even more to one third in the wet zone.

4.2.2 SMAP Evaluation based on Temperature Zones

The same analysis – time series analysis of seasonal variability, exploratory data analysis with box-and-whisker plots, and SMAP Soil Moisture product performance evaluation with the four statistical metrics – were made for the three temperature zones bordered along the lines of average annual temperature of 58 °F and 60°F respectively (Figure 8).



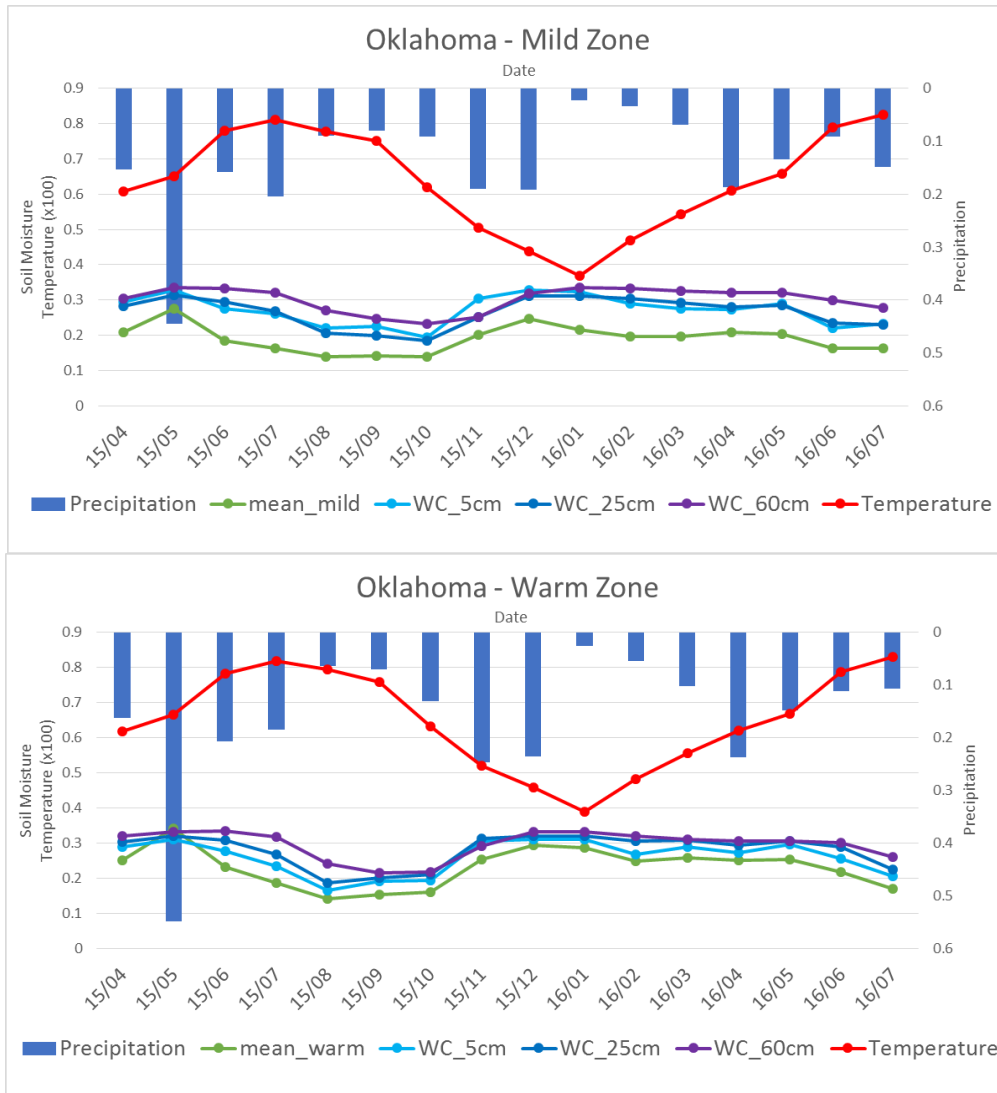


Figure 20 Time Series Analysis of Soil Moisture based on Temperature Zones

Again, soil water content, precipitation, and temperature follow a regular seasonal fluctuation and apparently interact with each other. The average monthly temperature of the three temperature zones didn't differ that much as the difference in the average monthly precipitation of the three precipitation zones, only varying more or less than one Fahrenheit degree between the adjacent zones. There is a noticeable increase of precipitation from the cool zone to the warm zone, so the main control factor may still be precipitation. However, since the temperature in Oklahoma fluctuates quite frequent, usually weekly or bi-weekly, it is presumed that temperature can be a

dominant factor for days and locations of low temperature during winter in the cool zone, or days and locations of high temperature during summer in the warm zone, which in both situations temperature controls the degree of evapotranspiration. The soil water content, in response to the varying precipitation and temperature, increased in a same manner with what is observed for precipitation zones from north to south, consistent with the latitudinal distribution of soil moisture analyzed in section 3.1 (Figure 11). SMAP retrievals follow the similar seasonal variation pattern with Mesonet observations, amongst which the closest with surface soil moisture, but in general underestimate soil water content than Mesonet with exceptions in the wet cool zones during the months of May, October, and November 2015 where there is a growing trend in precipitation, which was also the case for July 2016 in the wet zone when SMAP overestimated soil moisture than Mesonet. The changes in soil moisture is a tradeoff between increasing infiltration with rising precipitation and intensifying evapotranspiration rate by growing temperature. As can be captured from the July 2015 scenario in which both precipitation and temperature have risen, Mesonet can perceive immediate change in soil water content, where the surface moisture value of the month increases as a response to intensified precipitation, while SMAP, which relies on surface emission, or brightness temperature, to retrieve soil water content, is more sensible to temperature variation, as the soil moisture read has decreased for the month. In most cases SMAP reacted more strongly with changes in environmental conditions, such as extensive thunderstorms and tornadoes in May 2015 and dramatic decrease of precipitation within the mild zone in January 2016, than Mesonet. Therefore SMAP data can be considered a reliable indicator of the surface environmental conditions.

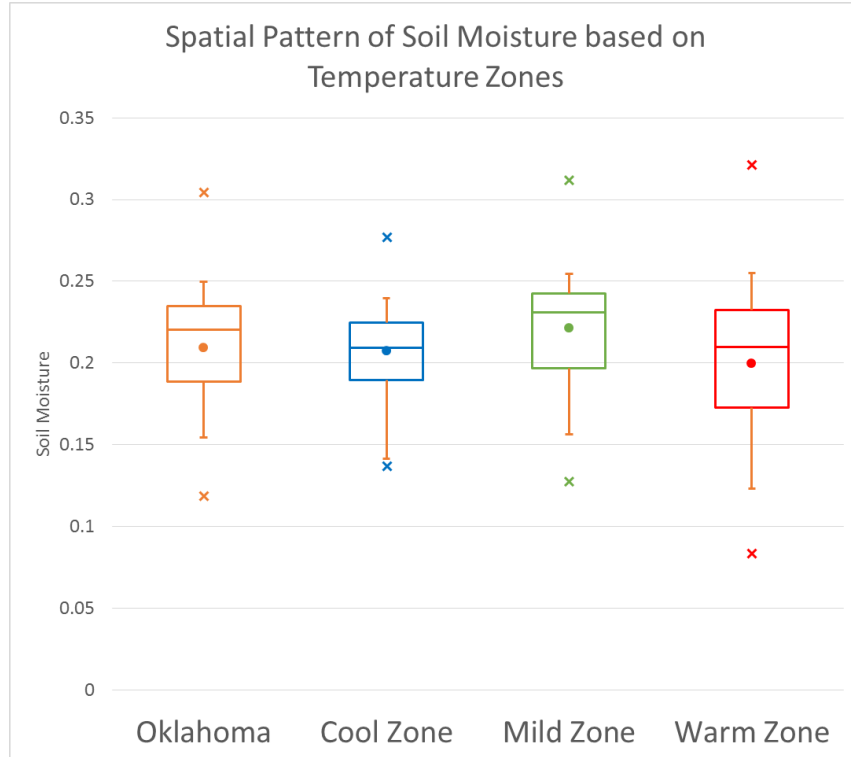


Figure 21 Box-and-Whisker Diagram for Each Temperature Zone

Box and whisker diagram plotted for the temperature zones has shown the maximum average soil water content within the mild zone in central Oklahoma, followed by the cool and warm zone. The warm zone has demonstrated the widest variation that exceeded $0.05 \text{ cm}^3 \cdot \text{cm}^{-3}$. Lower soil moisture level is attributed to less precipitation for the cool zone, and intense evapotranspiration due to higher temperature for the warm zone, respectively. The slight temperature difference may cause a widely varied evapotranspiration level due to diverged precipitation intensity, diverse vegetation type, soil texture, and other topographical elements, producing a deviated soil water content observed in the warm zone.

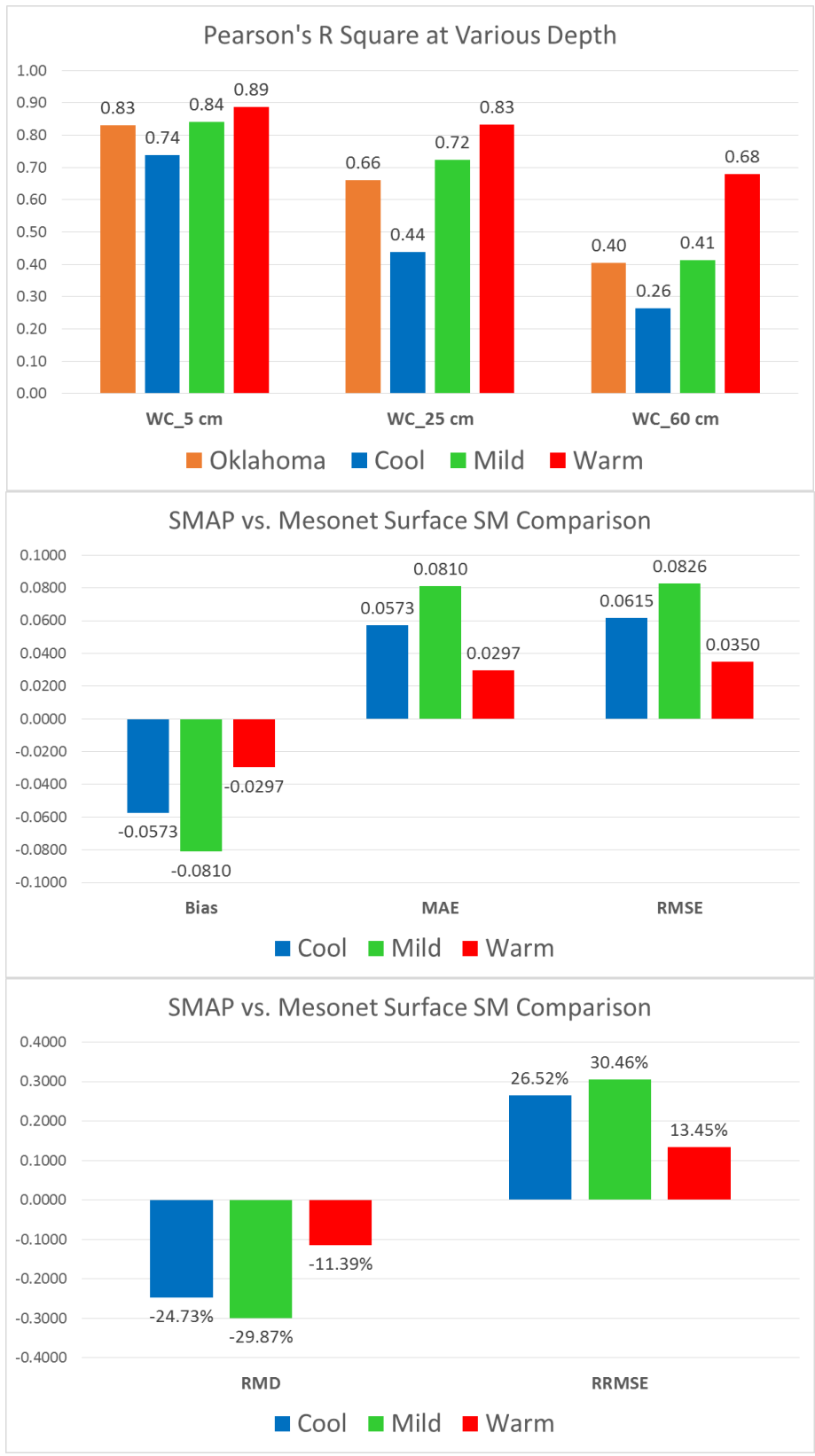
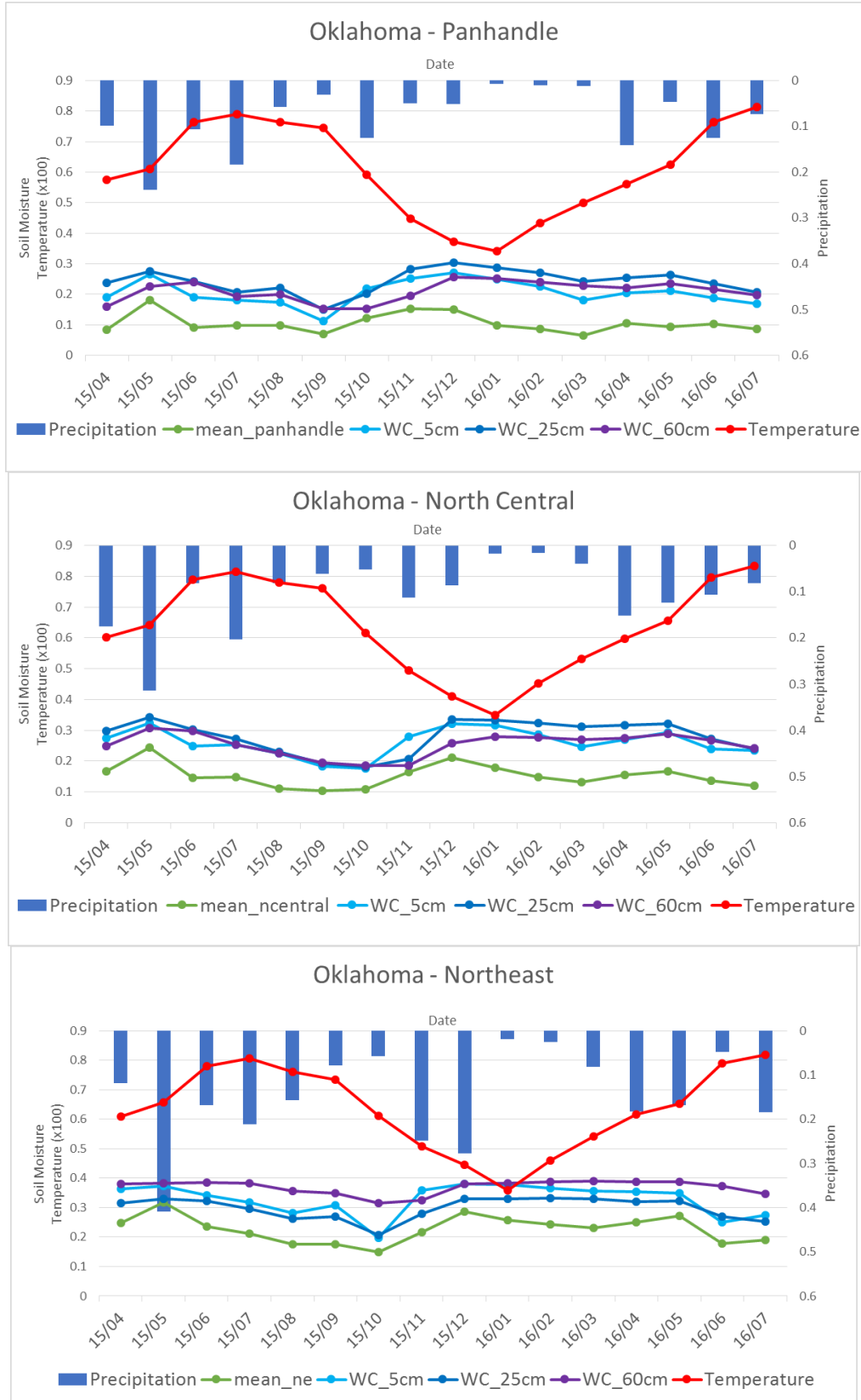
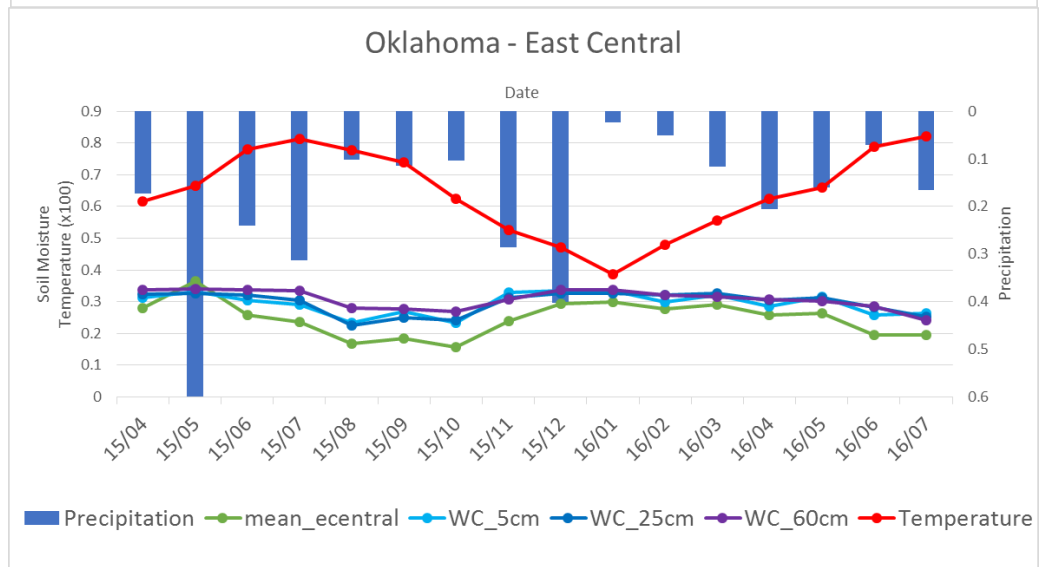
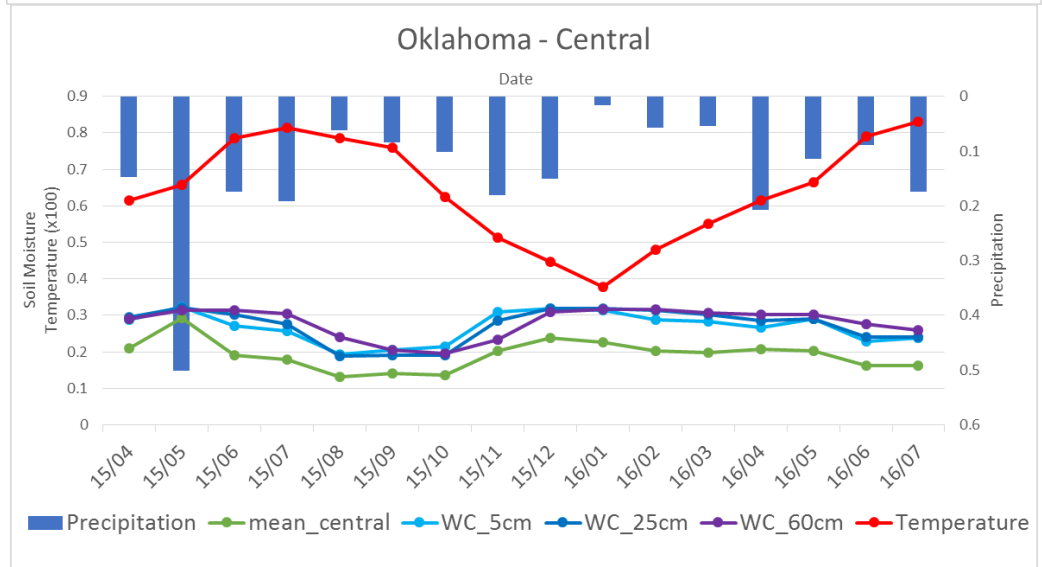
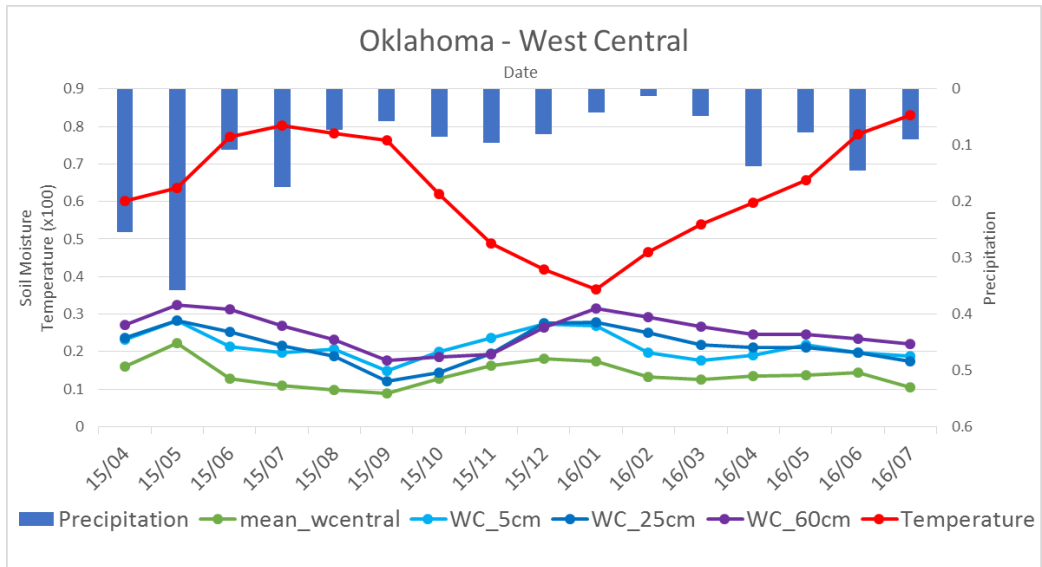


Figure 22 Statistics of SMAP – Mesonet Correlation for Each Temperature Zone

The Pearson's R^2 values have indicated a better correlation between SMAP retrievals and Mesonet observations from the cool zone to the warm zone, with remarkably strong association for surface soil water content with all R^2 values greater than 0.70 (Figure 22). Highest deviation is calculated in the mild zone where the highest soil water content was observed. Again the negative MD values indicate the underestimation of SMAP soil moisture retrievals than the Mesonet observations. The RRMSE values demonstrate that the error for the warm zone is half the level for the cool zone, which is 20% less than the mild zone. Therefore, conclusion can be made that SMAP soil moisture has a higher accuracy in the warm zone and relatively a lower accuracy in the cool zone (Figure 22).

4.2.3 SMAP Evaluation based on Climatic Divisions





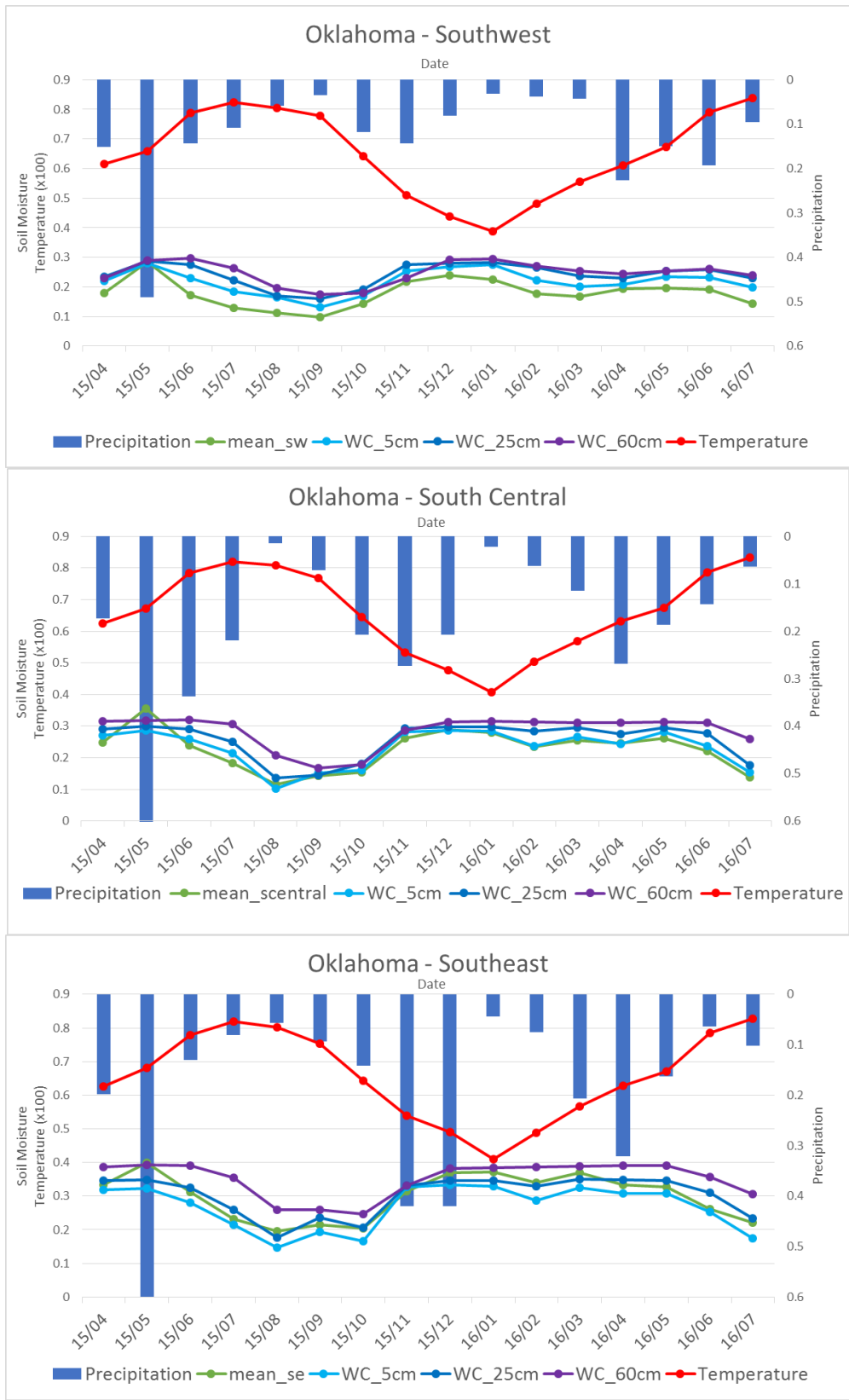


Figure 23 Time Series Analysis of Soil Moisture based on Climatic Regions

The time series analyses have shown an identical monthly variation pattern for average temperature across the state, while precipitation increases tremendously from the west to the east and from the north to the south directions, exerting spatial fluctuation of monthly average soil water content, which overall follows the precipitation pattern of high in the south and the east and low in the north and the west. Intense local rainfall events created enormous regional effects on soil moisture, including heavy rainfall during November-December 2015, which has raised the soil water content across the eastern Oklahoma. In general soil moisture fluctuated on a low level in the north and high in the south, but remained relatively stable in the east. In most cases root zone soil water content is higher than in the surface zone, with exceptions of observations at the 60-cm depth being the lowest in arid region during dry months. Comparing to the Mesonet observations, SMAP overall tends to underestimate soil moisture, but evidently overestimates surface soil moisture in the southeast portion of the state. The SMAP data show generally consistent monthly variation with the Mesonet data on the top layer. However, the SMAP data have shown a greater sensitivity to changes in surface environmental conditions including precipitation and temperature than the Mesonet data, which agrees with the findings over precipitation and temperature zones in previous sections.

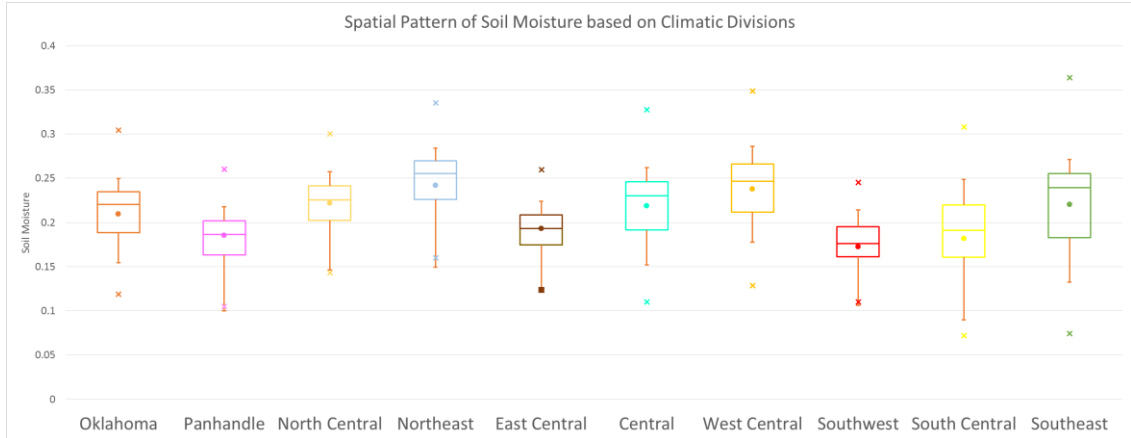


Figure 24 Box-and-Whisker Diagram for Each Climatic Region

It is clearly observed from the box-and-whisker plot that higher soil water content and wider deviation range are detected in the east and in the south. This is consistent with the results observed for precipitation and temperature zones, and matches the spatial distribution illustrated in longitudinal and latitudinal distributions of the Mesonet surface soil moisture (Figure 11) and statewide SMAP average monthly surface soil moisture (Figure 15, bottom-left). The widest data range greater than $0.06 \text{ cm}^3 \cdot \text{cm}^{-3}$ is spotted in southeastern Oklahoma where the highest level of soil moisture is measured. This is attributed to a combined effect of high precipitation increasing soil water content and high temperature withdrawing soil moisture.

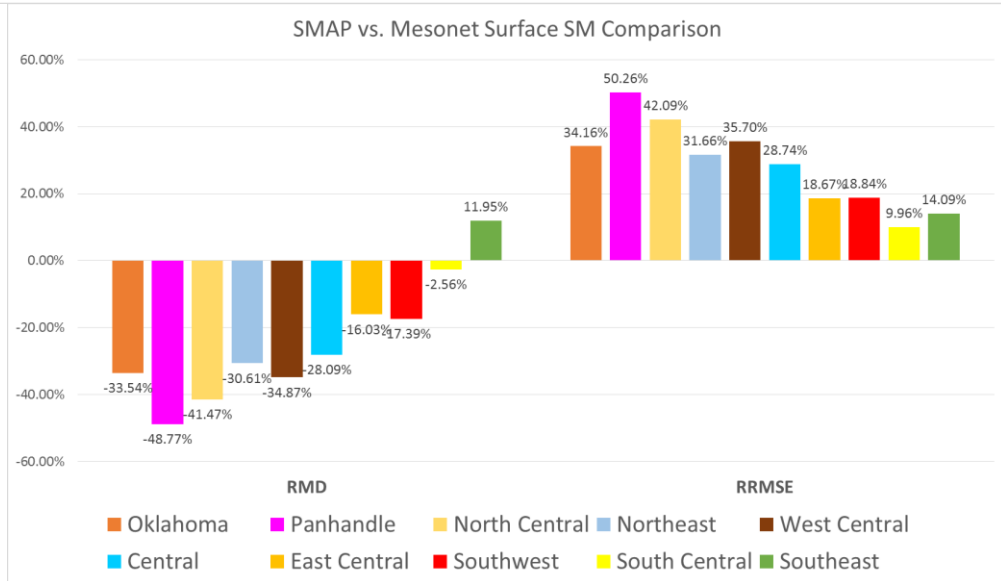
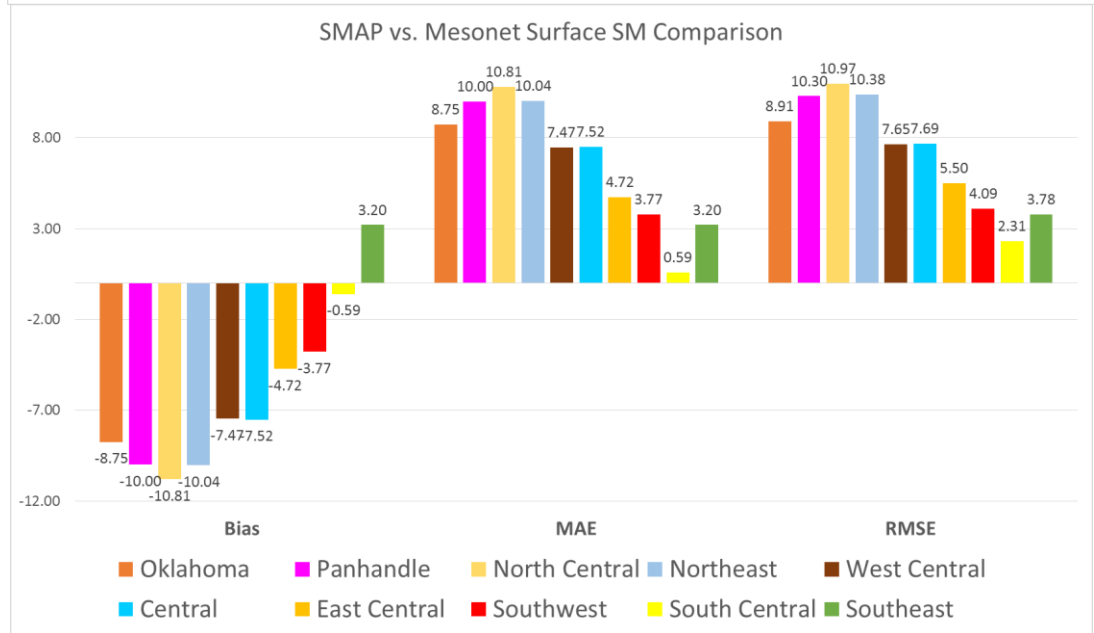
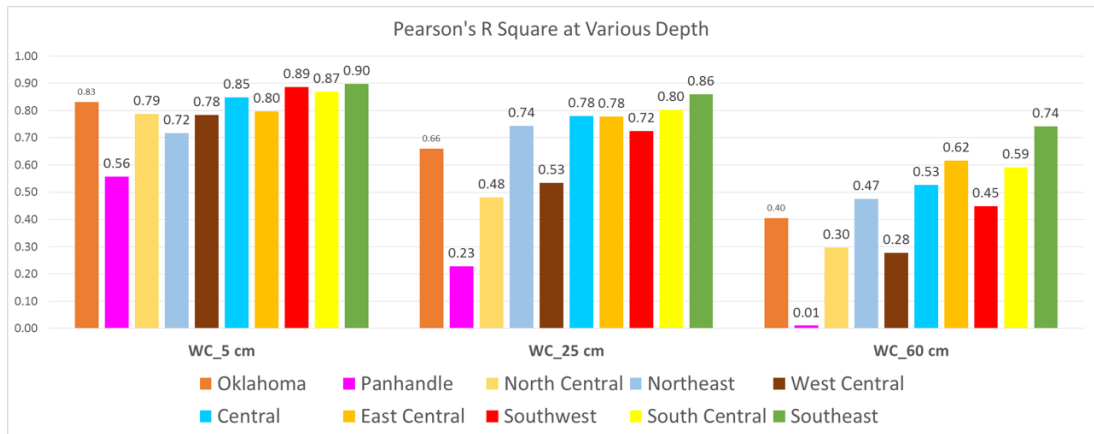


Figure 25 Statistics of SMAP – Mesonet Correlation for Each Climatic Region

In summary, statistics have shown high correlation and low differences between the SMAP retrievals and Mesonet observations in the east and in the south, and remarkably strong agreement between the two data sets for surface soil water content in the southern two thirds of the state with all R^2 values greater than 0.75. Deviation is high for root zone soil moisture measurements in the Panhandle area, which may due to the variations in infiltration and evapotranspiration rates as a result of heterogeneity of soil types. The negative values of MD or bias indicates that the SMAP soil moisture retrievals generally underestimate the soil moisture, with exception in southeastern Oklahoma, which is consistent with the findings in time series analysis. The RRMSE illustrates that the error overall shrinks from the west to the east and from the north to the south, except for the southeastern portion of the state. This may owe to the varied vegetation types which yields the deviation of reflection of remotely sensed signals, as well as the infiltration and evapotranspiration rates. This also explains the overestimation of SMAP products than Mesonet within the region, which is attributable to scattering and emission from vegetation.

Chapter 5. Temporal Analysis of SMAP Soil Moisture: *Seasonality*

In this chapter, I conducted the temporal variation analyses of the SMAP L3 soil moisture product by calculating grid-based seasonal average soil moisture value, computing the performance statistics on a grid-cell-by-grid-cell basis across the state, and conducting exploratory data analyses using methods like box-and-whisker plots. Due to the short and specific period, findings of the following seasonal patterns do not represent long-term climatology but just the 20-months hydrometeorology.

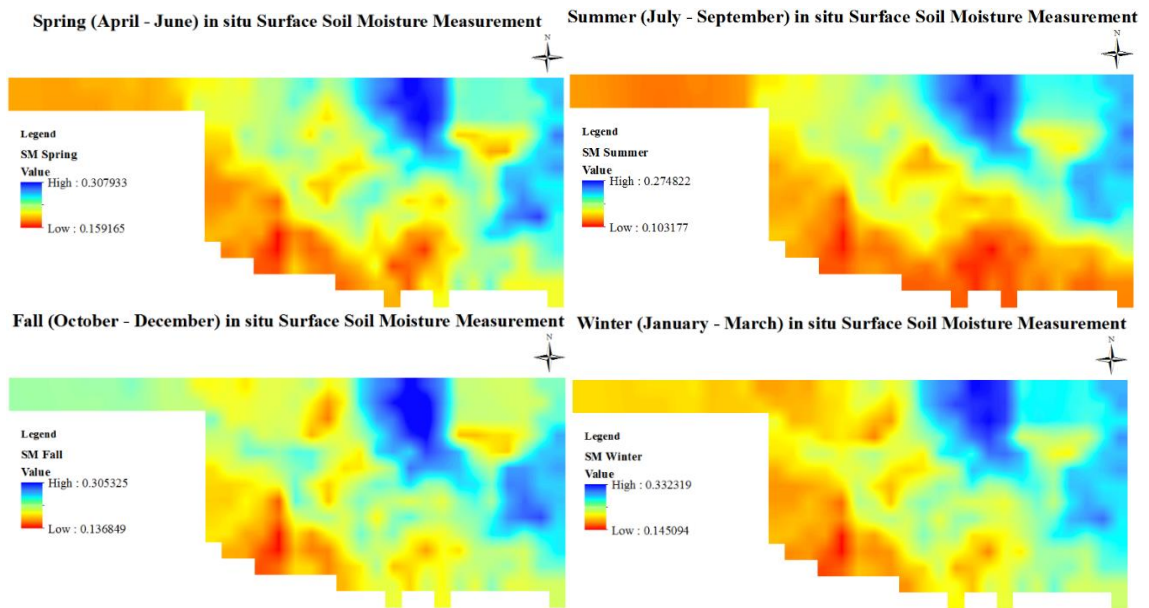


Figure 26 Average Seasonal Surface Soil Moisture Distribution

Grid-based average seasonal surface soil moisture was calculated with interpolated Mesonet monthly data and spatially plotted in Figure 26. The dry summer in 2016 (July – September) witnessed the lowest soil water contents, while the relatively wet winter (January – March) had the highest values (Figure 26). These results are

consistent with the above findings from the time series analyses. Additionally, evident regional fluctuation is observed for panhandle region, deviating from low values in summer to high values in fall. The seasonal fluctuation results from an additive effect of precipitation and temperature—precipitation starts to decrease and temperature reaches to its peak in summer, significantly reducing the soil water content.

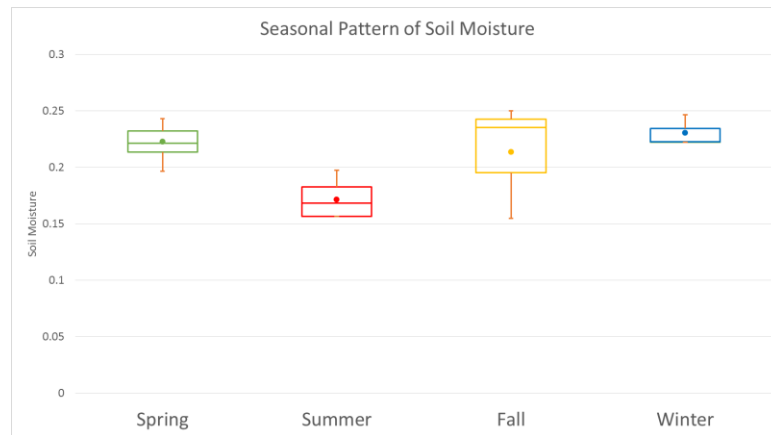
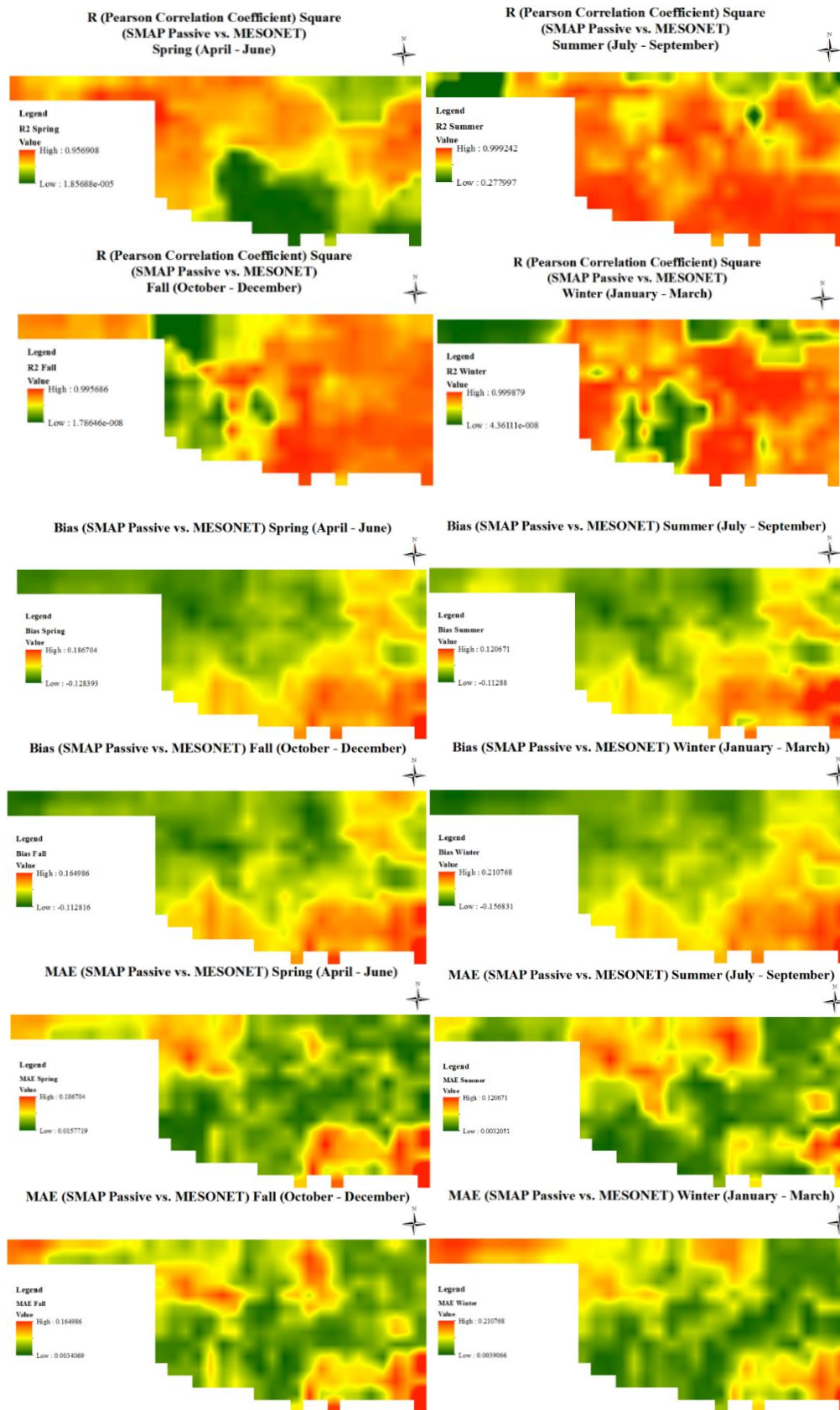


Figure 27 Box-and-Whisker Diagram for Each Season

To quantitatively measure the fluctuation, the box-and-whisker diagram is plotted. The seasonal variation pattern from the exploratory data analyses agreed with the results of time series analyses: soil water content value reaching the lowest in summer, the highest in winter, and the largest variation in fall. The median value in fall exceeds the mean by 10%, indicating the soil water content level is spread around the upper quartile, maintaining at a relatively high value.

The four statistical metrics of the SMAP retrievals relative to the Mesonet observations are calculated at each grid cell for each season and plotted in Figure 28.



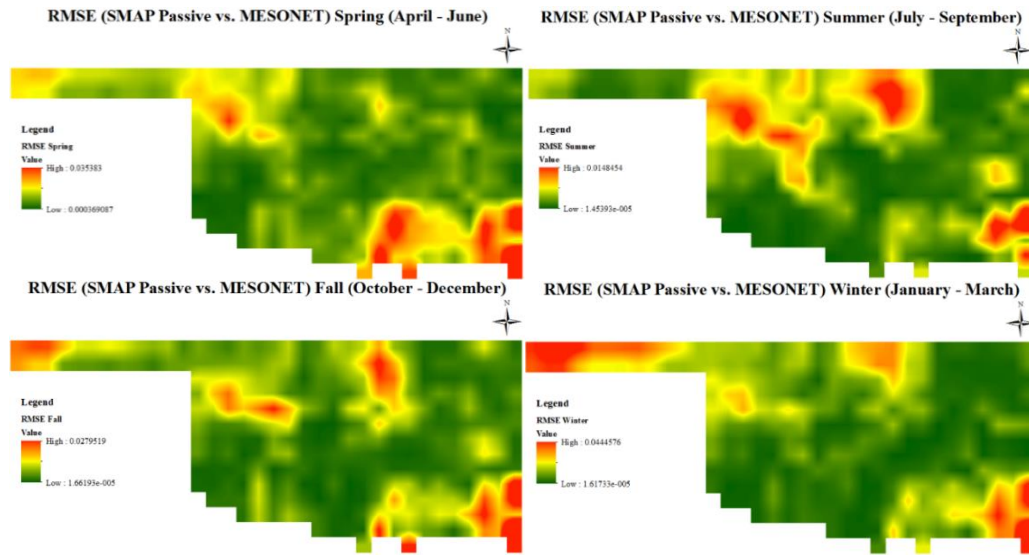


Figure 28 Statistics for SMAP – Mesonet Correlation Statewide

Pearson’s R^2 shows a high correlation throughout the state all year round, with exception in southern Oklahoma during spring. This may be the result of the deviation between precipitation-sensitive Mesonet and temperature-derived SMAP soil moisture data. Intense precipitation events during May increases soil moisture values but reduces surface temperature and lowers SMAP reads, whereas the growing temperature and declining rainfall reduces soil water content – but increases SMAP measurements. Bias values have suggested an underestimate of the SMAP retrievals relative to the Mesonet observations, whilst overestimation happens in the southeastern Oklahoma, consistent with the spatial pattern found for climatic divisions. Error is constantly low (< 0.05) all across the state throughout the year but relatively high in the southeastern tip of the state, possibly produced by the tradeoff between antagonistic effects of precipitation and temperature.

Chapter 6. Summary, Conclusions and Future Work

6.1 Summary and Conclusions

In this study, the spatiotemporal variation patterns of soil moisture in Oklahoma were studied. The quality of remotely sensed SMAP L3 soil moisture product was evaluated using the observations of the environmental monitoring network Mesonet across the state. Spatial variation patterns of the SMAP data and their degree of agreement with the Mesonet observations were analyzed. This was done in terms of climatic conditions based on average annual precipitation and temperature distributions. For the above comparison, I divided the state of Oklahoma into three precipitation zones, three temperature zones, and nine climatic regions as a combination of precipitation and temperature effects. Temporal patterns were explored on both monthly and seasonal time scales. For each climatological region and each season respectively the following procedures were performed: time series analysis of seasonal variability, exploratory data analysis with box-and-whisker plots, and the performance evaluation of the SMAP Soil Moisture product with the four statistical metrics. The spatial and temporal observations of the soil moisture variation patterns in the state of Oklahoma have yielded a considerable knowledge on satellite measurements of soil water content. Based on the evaluations and analyses, findings are concluded as follows:

1: The remotely sensed SMAP retrievals well fit and were highly correlated with ground-observed Oklahoma Mesonet data, both spatially and temporally. Spatially, the wetter and the warmer climatic condition yielded a higher correlation and lower error between SMAP retrievals and Mesonet observations. Temporally, both summer and winter exhibited greater degree of deviations than the rest of the year, as a result of antagonistic effect by infiltration and evapotranspiration events.

2: The Mesonet ground data of depth at the top 5 cm have shown the best correlation with the SMAP information, which demonstrates that the remotely sensed SMAP data will be more valid for measuring the topsoil layer than root zone soil moisture, as a result of remote sensing signal penetration blockage by the ground.

3: Remotely sensed SMAP soil moisture corresponded with changes in surface environmental conditions, especially with climatic events of precipitation and temperature variation.

Overall, this study proves the hypotheses and concludes that the remote sensed soil moisture data retrieved from SMAP is considered be effective in observing land surface soil moisture data in Oklahoma.

6.2 Future Work

This work has utilized a methodological framework and provided an example for future work on remote sensing soil moisture evaluation products. More factors are to be considered including surface conditions of surface roughness, soil texture, and vegetation types. Moreover, other remote sensing products should be considered including ESA's Soil Moisture and Ocean Salinity (SMOS) mission and JAXA's Advanced Microwave Scanning Radiometer (AMSR)-2. The knowledge acquired from the current and future research in comparison of remotely sensed soil moisture data with ground observation can assist electrical engineers calibrate the error in remote sensing signals and retrieval signals, and thus to develop more functional satellite sensors for future missions.

References

1. Bi, Haiyun, Jiangyuan Zeng, Wenjun Zheng and Xiwei Fan, "Validation of SMAP Soil Moisture analysis product using in-situ measurements over the Little Washita Watershed," 2016 IEEE International Geoscience and Remote Sensing Symposium (IGARSS), Beijing, 2016, pp. 3086-3089.
2. Bindlish, Rajat, Thomas J. Jackson, Eric Wood, Huilin Gao, Patrick Starks, David Bosch, and Venkat Lakshmi. "Soil Moisture Estimates from TRMM Microwave Imager Observations over the Southern United States." *Remote Sensing of Environment* 85.4 (2003): 507-15. Print.
3. Brock, Fred V., Kenneth C. Crawford, Ronald L. Elliott, Gerrit W. Cuperus, Steven J. Stadler, Howard L. Johnson, and Michael D. Eilts. "The Oklahoma Mesonet: A Technical Overview." *Journal of Atmospheric and Oceanic Technology* 12.1 (1995): 5-19.
4. Charpentier, Michael A., and Peter M. Groffman. "Soil moisture variability within remote sensing pixels." *Journal of Geophysical Research*, 97.D17 (1992): 18987.
5. Chen, Jiongfeng. "Validation of Passive Microwave Remotely Sensed Soil Moisture (Amsr-E) Products in the Yihe Catchment, Shandong Province of China." *International Journal of Engineering Research and Applications* 6.11 (2016): 80-84.
6. Crow, Wade T., Aaron A. Berg, Michael H. Cosh, Alexander Loew, Binayak P. Mohanty, Rocco Panciera, Patricia Rosnay, Dongryeol Ryu, and Jeffrey P. Walker. "Upscaling Sparse Ground - based Soil Moisture Observations for the Validation of Coarse - resolution Satellite Soil Moisture Products." *Reviews of Geophysics* 50.2 (2012).

7. Draper, Clara S., Jeffrey P. Walker, Peter J. Steinle, Richard A.m. De Jeu, and Thomas R.h. Holmes. "An Evaluation of AMSR–E Derived Soil Moisture over Australia." *Remote Sensing of Environment* 113.4 (2009): 703-10. Print.
8. Fan, Yun. "Climate Prediction Center Global Monthly Soil Moisture Data Set at 0.5° Resolution for 1948 to Present." *Journal of Geophysical Research* 109.D10 (2004).
9. Gao, Huilin. *Passive Microwave Remote Sensing of Surface Soil Moisture: Methods, Results, and Applications*. Diss. Princeton U, 2005. Print.
10. Illston, Bradley G., Jeffrey B. Basara, Christopher A. Fiebrich, Kenneth C. Crawford, Eric Hunt, Daniel K. Fisher, Ronald Elliott, and Karen Humes. "Mesoscale Monitoring of Soil Moisture across a Statewide Network." *Journal of Atmospheric and Oceanic Technology* 25.2 (2008): 167-82.
11. Jin, Menglin S., and Mullens, Terrence. "A Study of the Relations between Soil Moisture, Soil Temperatures and Surface Temperatures Using ARM Observations and Offline CLM4 Simulations." *Climate2.4* (2014): 279-95.
12. Liu, Wenjuan, Yang Hong, Sadiq Khan, Mingbin Huang, Trevor Grout, and Pradeep Adhikari. "Evaluation of Global Daily Reference ET Using Oklahoma's Environmental Monitoring Network—MESONET." *Water Resour Manage* 25.6 (2011): 1601-613. Print.
13. McCorkle, Taylor A, Skylar S Williams, Timothy A Pfeiffer, and Jeffrey B Basara. "Atmospheric Contributors to Heavy Rainfall Events in the Arkansas-Red River Basin." *Advances in Meteorology* 2016 (2016): 15.
14. "Mesonet." Mesonet. Web. 22 Feb. 2016.

15. Miller and Fox. "A Tool for Drought Planning in Oklahoma: Estimating and Using Drought-influenced Flow Exceedance Curves." *Journal of Hydrology: Regional Studies* 10 (2017): 35-46.
16. Miralles, Diego G., Wade T. Crow, and Michael H. Cosh. "Estimating Spatial Sampling Errors in Coarse-Scale Soil Moisture Estimates Derived from Point-Scale Observations." *Journal of Hydrometeorology* 11.6 (2010): 1423-429.
17. Mohanty and Skaggs. "Spatiotemporal Evolution and Time-stable Characteristics of Soil Moisture within Remote Sensing Footprints with Varying Soil, Slope, and Vegetation." *Advances in Water Resources* 24.9 (2001): 1051-067.
18. Pandey, Vanita, and Pandey, Pankaj K. "Spatial and Temporal Variability of Soil Moisture." *International Journal of Geosciences* 01.02 (2010): 87-98.
19. Peel, M. C., Finlayson, B. L., and McMahon, T. A.. "Updated World Map of the Köppen-Geiger Climate Classification." *Hydrology and Earth System Sciences* 11.5 (2007): 1633-644.
20. Shen, Xinyi, Kebiao Mao, Qiming Qin, Yang Hong, and Guifu Zhang. "Bare Surface Soil Moisture Estimation Using Double-Angle and Dual-Polarization L-Band Radar Data." *IEEE Transactions on Geoscience and Remote Sensing* 51.7 (2013): 3931-942.
21. "SMAP: Soil Moisture Active Passive." SMAP. Web. 22 Feb. 2016.
22. "SMAP L3 Radar Global Daily 3 km EASE-Grid Soil Moisture, Version 3." National Snow and Ice Data Center. Web. 22 Feb. 2016.
23. Tian, Zhengchao, Li, Zizhong, Liu, Gang, Li, Baoguo, and Ren, Tusheng. "Soil Water Content Determination with Cosmic-ray Neutron Sensor: Correcting

- Aboveground Hydrogen Effects with Thermal/fast Neutron Ratio." *Journal of Hydrology* 540 (2016): 923-33.
24. "USGS - CEGIS - Soil Moisture." USGS - CEGIS - Soil Moisture. Web. 22 Feb. 2016.
25. Wang, Mo, Liu, Lin, and Hu. "Validation and Trend Analysis of ECV Soil Moisture Data on Cropland in North China Plain during 1981–2010." *International Journal of Applied Earth Observations and Geoinformation* 48 (2016): 110-21.
26. Wang, Xianwei, French, Richard, Keating, Jerome, Murray, Kyle, Sharif, Hatim, and Xie, Hongjie. *Applications of Remote Sensing and GIS in Surface Hydrology: Snow Cover, Soil Moisture and Precipitation* (2008): ProQuest Dissertations and Theses.
27. Werner, Hal. "Measuring Soil Moisture for Irrigation Water Management." SDSU College of Agriculture & Biological Sciences Publications (1992). Print.
28. Wu, Liu, Wang, and Deng. "Evaluation of AMSR2 Soil Moisture Products over the Contiguous United States Using in Situ Data from the International Soil Moisture Network." *International Journal of Applied Earth Observations and Geoinformation* 45 (2016): 187-99.
29. Yao, Xueling, Fu, Bojie, Lu, Yihe, Sun, Feixiang, Wang, Shuai, and Liu, Min. "Comparison of Four Spatial Interpolation Methods for Estimating Soil Moisture in a Complex Terrain Catchment." *PLoS ONE* 8.1 (2013): E54660.
30. Yuan, Shanshui, and Steven M. Quiring. "Comparison of Three Methods of Interpolating Soil Moisture in Oklahoma." *International Journal of Climatology* 37.2 (2017): 987-97.

31. Zhang, Xuefei, Zhang, Tingting, Zhou, Ping, Shao, Yun, and Gao, Shan. "Validation Analysis of SMAP and AMSR2 Soil Moisture Products over the United States Using Ground-Based Measurements." *Remote Sensing* 9.2 (2017): 104.

32. Zhang, Yu, Yang Hong, Xuguang Wang, Jonathan J. Gourley, Jidong Gao, Humberto J. Vergara, and Bin Yong. "Assimilation of Passive Microwave Streamflow Signals for Improving Flood Forecasting: A First Study in Cubango River Basin, Africa." *IEEE Journal of Selected Topics in Applied Earth Observations and Remote Sensing* 6.6 (2013): 2375-390. Print.]